Karlsruhe Institute of Technology

Different methods to derive the mixing-layer height by remote sensing (including RASS)

Stefan Emeis
stefan.emeis@kit.edu

INSTITUTE OF METEOROLOGY AND CLIMATE RESEARCH, Atmospheric Environmental Research

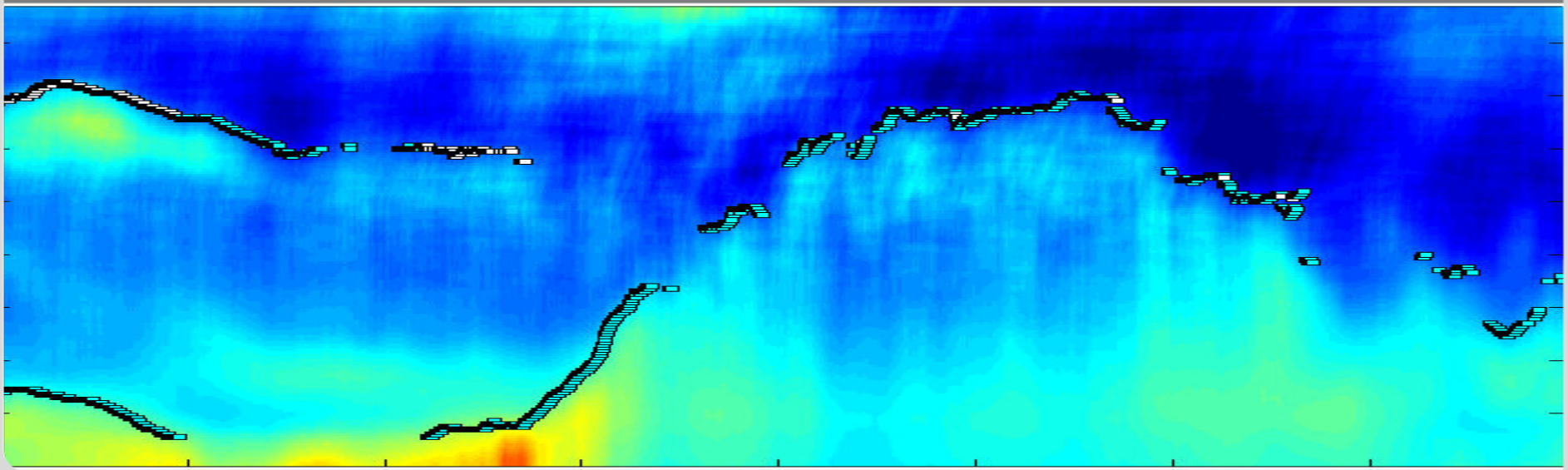

Introduction

- definition of mixing layer

- relevance for wind energy

- remote sensing

stefan.emeis@kit.edu Institute for Meteorology and Climate Research – Atmospheric Environmental Research

Mixing-layer height

Inversion height	literally: inversion in the temperature profile, increase of temperature with height, strong decrease of moisture, radiation inversions, sinking inversions, surface inversions, lifted inversions
Mixing-layer height (mixing height, mixed-layer height)	upper boundary for vertical exchange (mixing), upper boundary of the well-mixed layer, entrainment, defined by the turbulence profile or by the vertical distribution of a tracer (aerosol, pot. temperature)
Boundary layer height	SBL: at night, height of the near-surface layer influenced by surface friction CBL: at day, height of convective plumes

boundary layer height $\approx$ mixing-layer height

boundary layer height $\geq$ inversion height

Mixing-layer height influences diurnal variation of vertical wind profiles

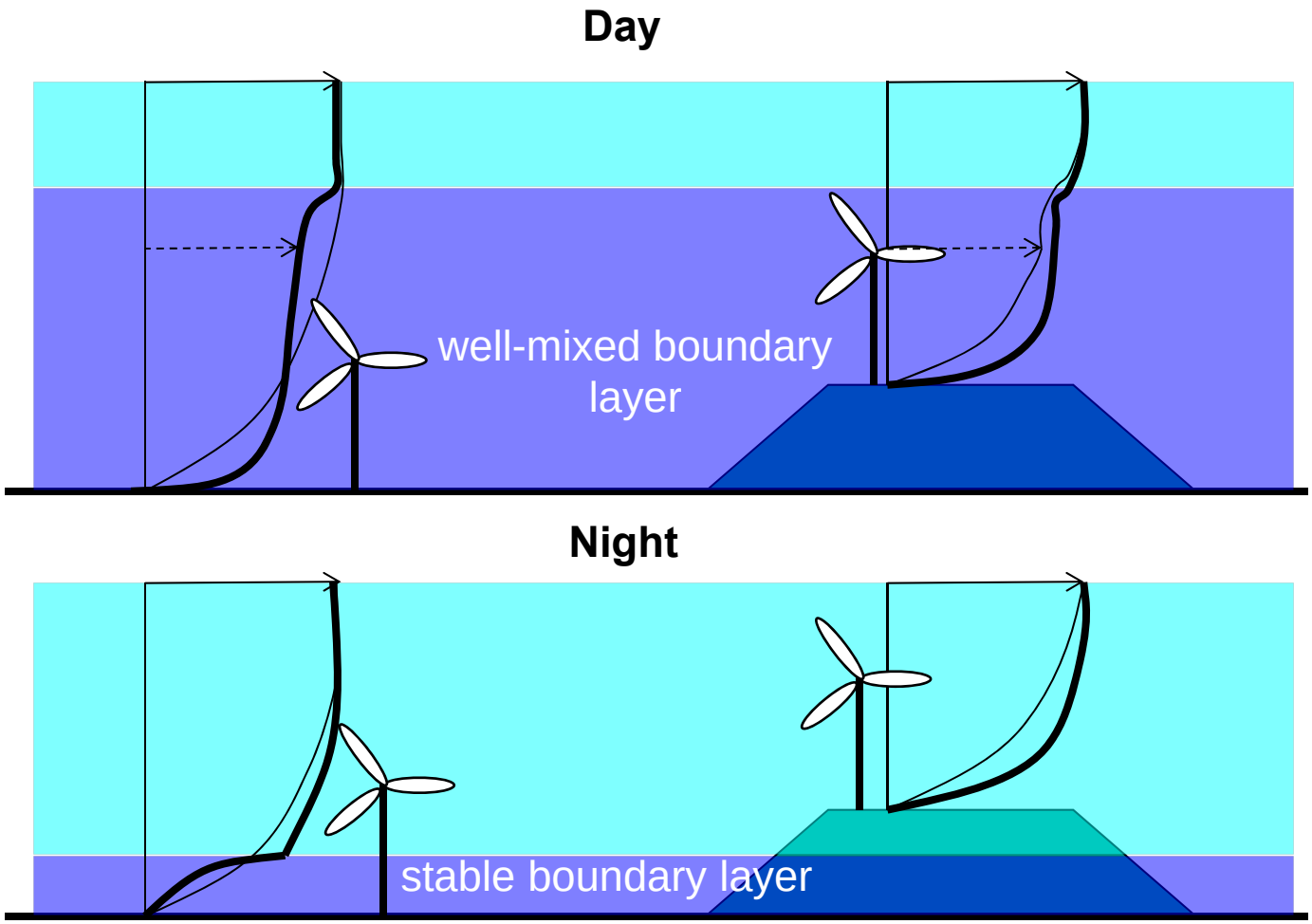

Nocturnal low-level jet and the turning of wind direction with height

Day

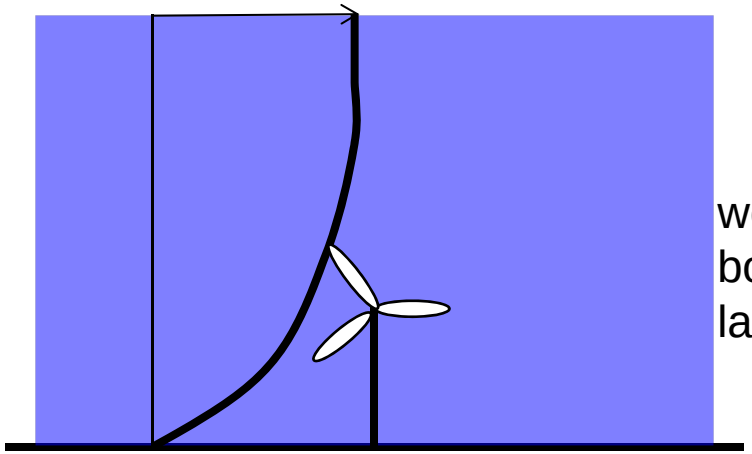

well-mixed boundary layer

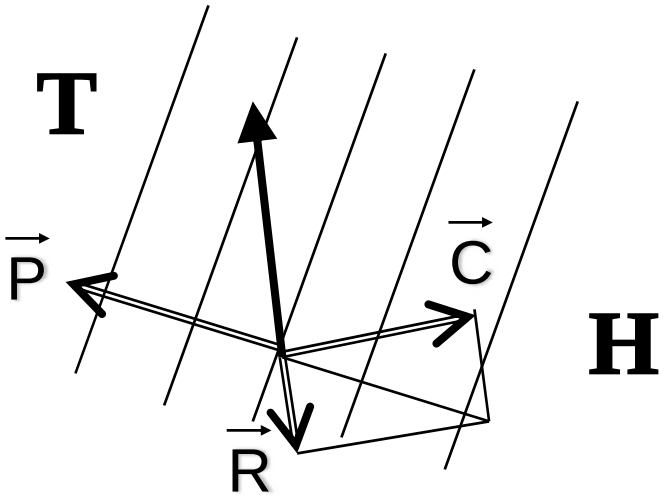

Night

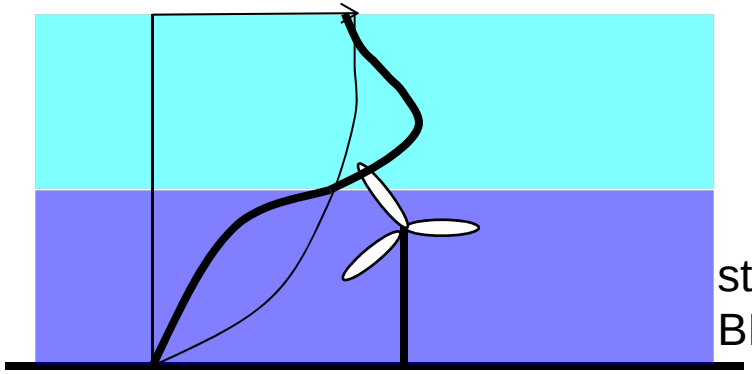

stable BL

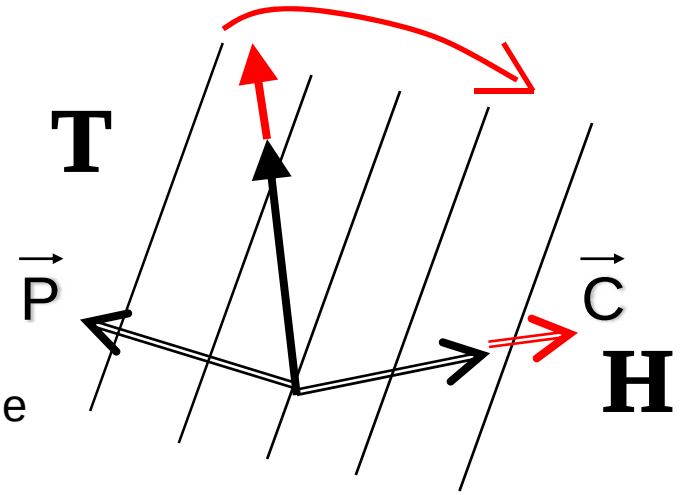

Mean diurnal variation of the turning of wind direction with height

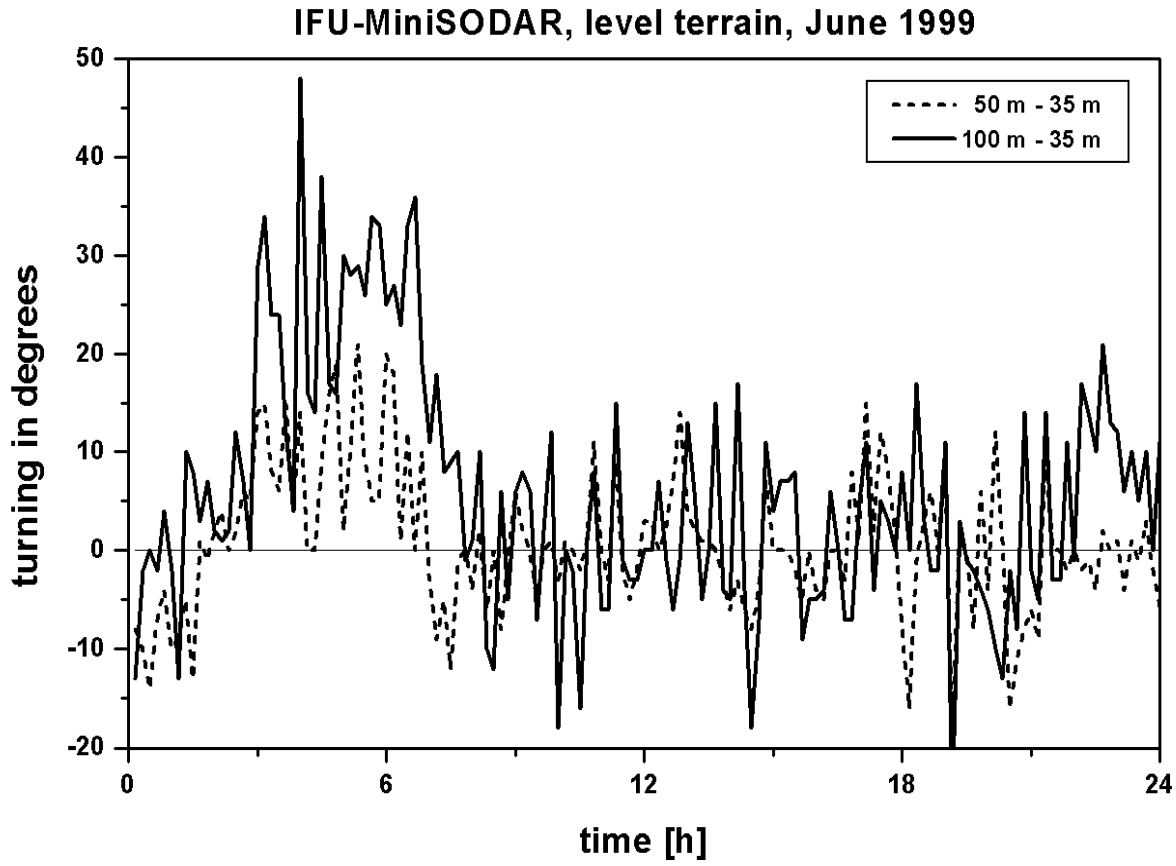

Emeis, S., 2001: Vertical variation of frequency distributions of wind speed in and above the surface layer observed by sodar. Meteorol. Z., **10**, 141-149.

example for extreme turning of wind direction with height

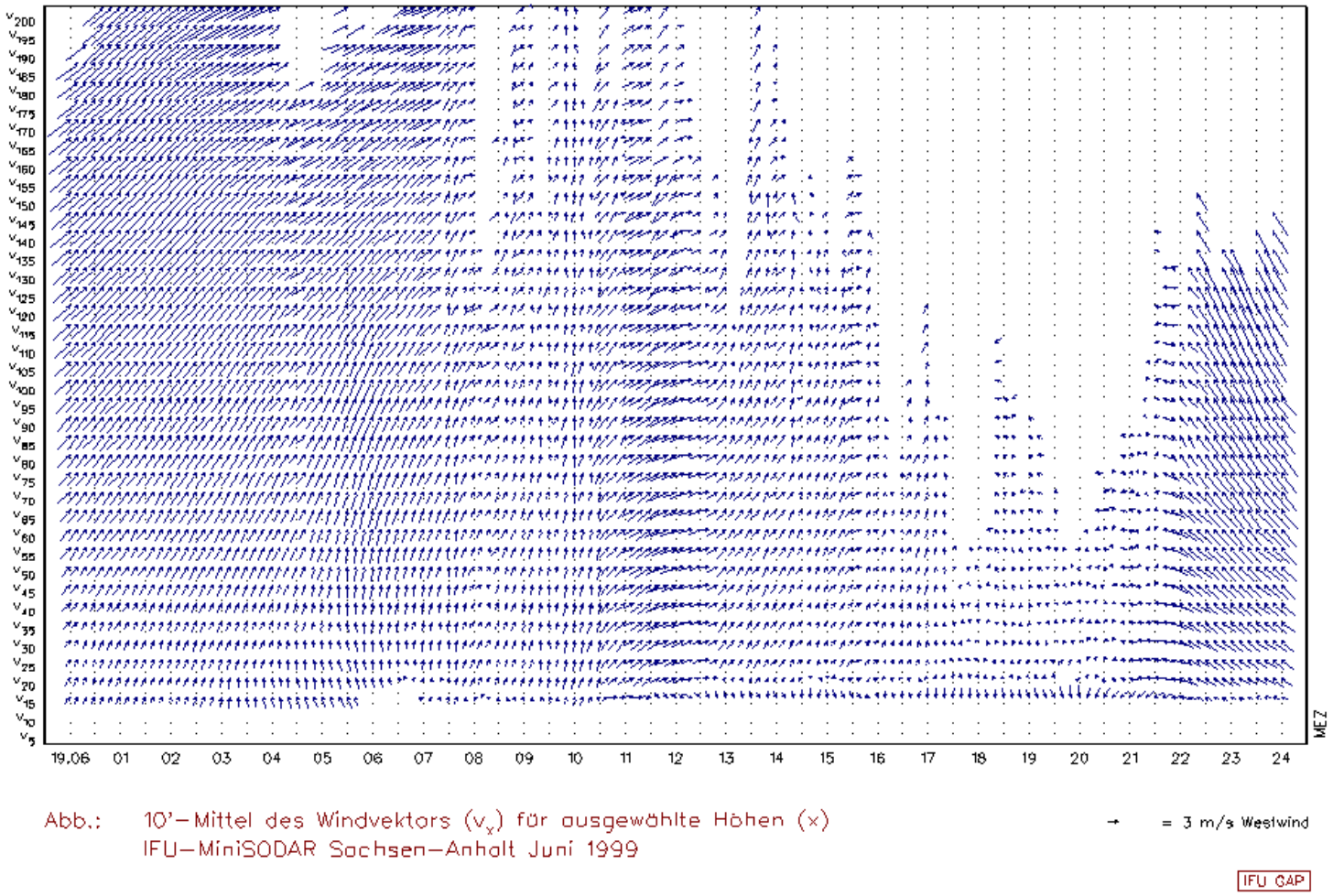

Emeis, S., 2001: Vertical variation of frequency distributions of wind speed in and above the surface layer observed by sodar. Meteorol. Z., **10**, 141-149.

The vertical wind profile

logarithmic law
(with stability correction) $u(z) = (u_*/\kappa)\,(\ln(z/z_0) - \psi(z/L_*))$

power law $u(z) = u(z_A)\,(z/z_A)^n$

New proposal
(Gryning et al. 2007)

$$u(z) = \frac{u_{*0}}{\kappa}\left(\ln\left(\frac{z}{z_0}\right) + \frac{z}{L_{MBL,N}} - \frac{z}{z_i}\left(\frac{z}{2L_{MBL,N}}\right)\right)$$

needs information on the PBL or mixing-layer height

Gryning, S.-E., E. Batchvarova, B. Brümmer, H. Jørgensen, S. Larsen, 2007: On the extension of the wind profile over homogeneous terrain beyond the surface boundary layer. Bound.-Lay. Meteorol., **124**, 251–268.

Peña, A., S.-E. Gryning, C.B. Hasager, 2010: Comparing mixing-length models of the diabatic wind profile over homogeneous terrain. Theor. Appl. Climatol., **100**, 325-353.

Basic remote sensing techniques

subject of this lecture

name	princple	spatial resolution	direction	type
RADAR	backscatter, electro-magnetic pulses, fixed wave length	profiling	scanning, slanted	active, monostatic
SODAR	backscatter, acoustic pulses, fixed wave length	profiling	fixed, slanted, vertical	active, usually monostatic
LIDAR	backscatter, optical pulses, fixed wave length(s)	profiling	scanning, fixed, horizontal, slanted, vertical	active, monostatic
RASS	backscatter, acoustic, electro-magnetic, fixed wave length	profiling	fixed, vertical	active, monostatic
FTIR	absorption, infrared, spectrum	path-averaging	fixed, horizontal, slanted	active, bistatic or passive
	emission, infrared, spectrum	path-averaging	fixed, horizontal, slanted	passive
DOAS	absorption, optical, fixed wave lengths	path-averaging	fixed, horizontal	active, bistatic
radiometry	electro-magnetic, fixed wave length(s)	averaging, profiling	fixed, scanning, slanted, vertical	passive
tomography	travel time, acoustic, fixed wave length	horizontal distribution	fixed, horizontal	active, multiple emitters and receivers

subject of this lecture

Frequencies for atmospheric remote sensing

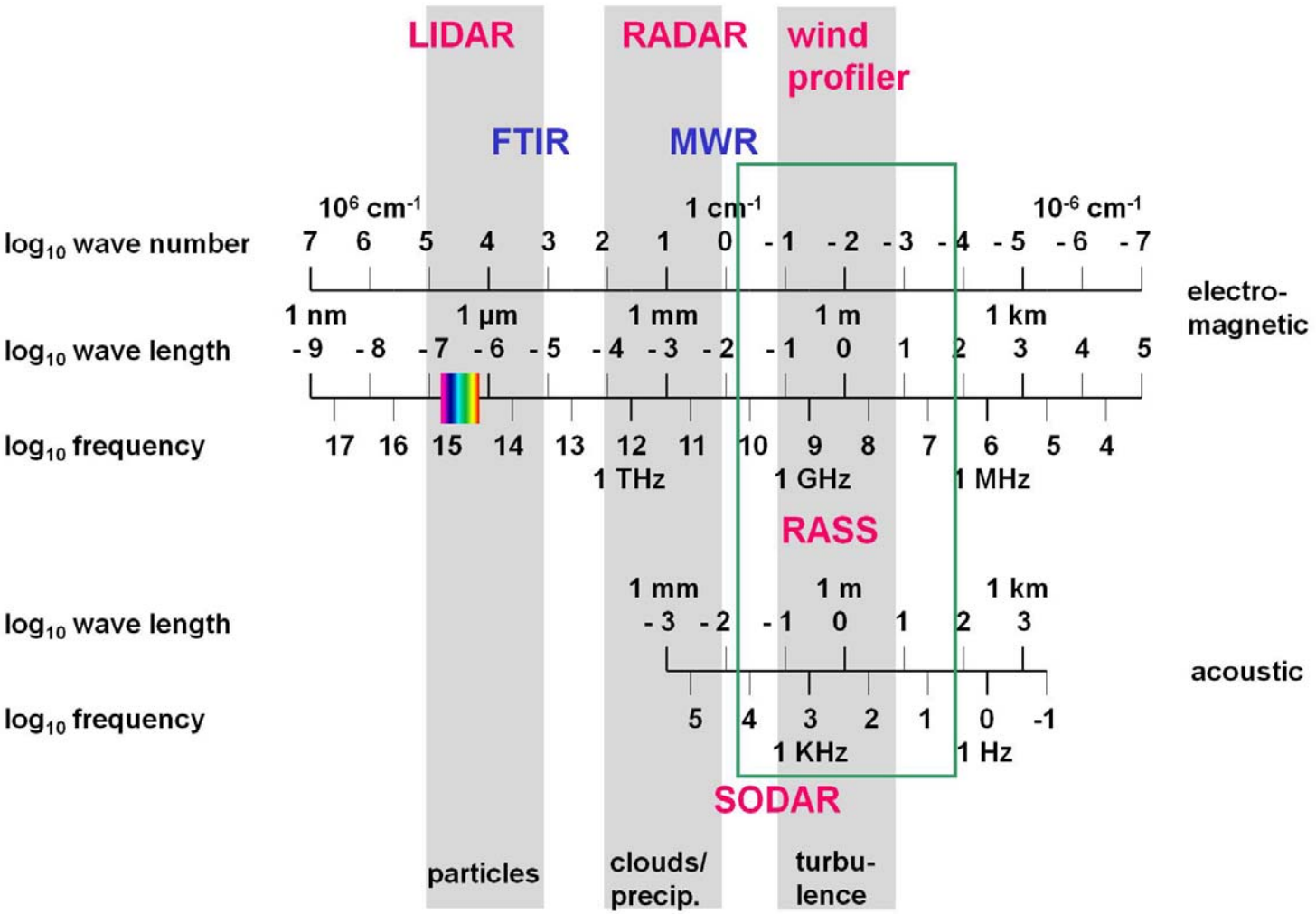

Emeis, S., 2010: Measurement Methods in Atmospheric Sciences - In situ and remote. Borntraeger, Stuttgart, 272 pp., 103 figs, 28 tables, ISBN 978-3-443-01066-9.

SODAR

algorithms for the determination of mixing-layer height

stefan.emeis@kit.edu Institute for Meteorology and Climate Research – Atmospheric Environmental Research

monostatic SODAR: measuring principles

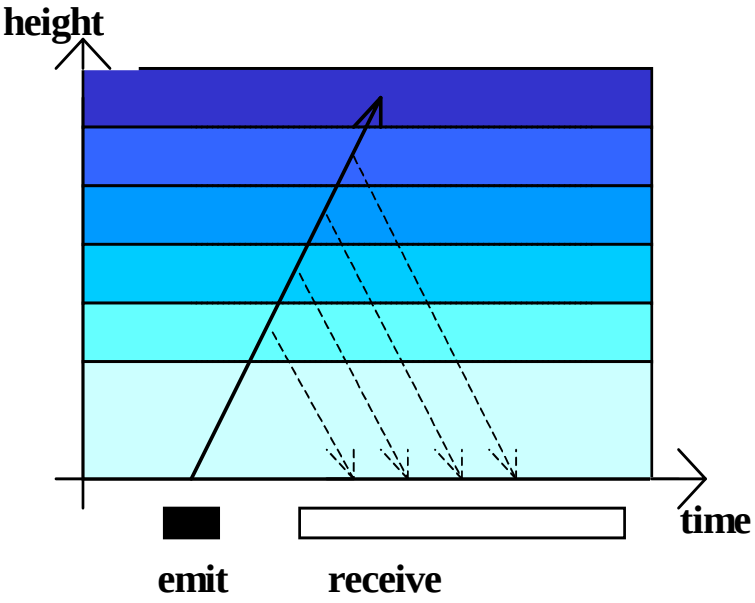

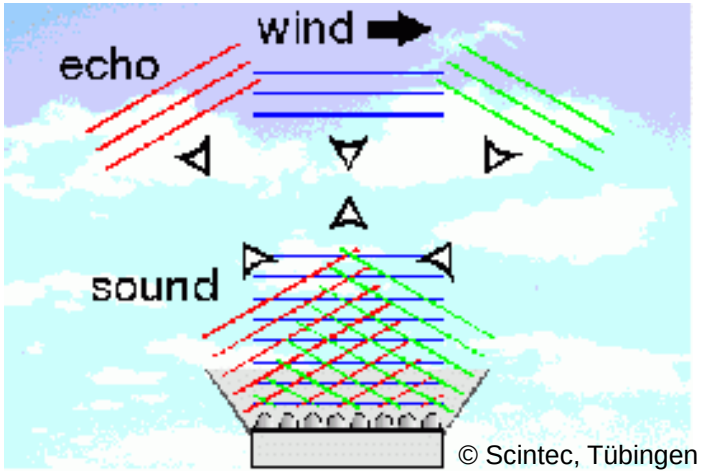

deduction:

sound travel time	=	height
backscatter intensity	=	turbulence
Doppler-shift	=	wind speed

Emission of sound waves into three directions:

in order to measure all three components of the wind (horizontal and vertical)

The SODAR equation:

$$P_R = r^2 (c_s \tau A \varepsilon/2) P_0 \beta_s e^{-2\sigma r} + P_{bg}$$

P_R received power,
P_0 emitted power,
ε antenna efficiency,
A effective antenna area,
σ sound absorption in air due to classical and molecular absorption due to the collision of water molecules with the oxygen and nitrogen molecules of the air,
r distance between the scattering volume and the instrument,
τ pulse duration (typically between 20 and 100 ms),
β_s backscattering cross-section (typically in the order of 10^{-11} m^{-1} sr^{-1}),
c_s sound speed,
P_{bg} background noise.

Emitted power: ~ 10^3 W, received (backscattered) power: 10^{-15} W

The SODAR equation:

$$P_R = r^{-2} (c_s \tau A \varepsilon/2) P_0 \beta_s e^{-2\sigma r} + P_{bg}$$

The ratio of the two terms on the right-hand side of the SODAR equation is called signal-to-noise ratio (usually abbreviated as SNR).

The backscattering cross-section β_s is a function of the temperature structure function C_T^2 (Tatarskii 1961).

For a monostatic SODAR we find (Reitebuch 1999) when using the wave number k = 2π/λ:

$$\beta_s(180°) = 0{,}00408\, k^{1/3}\, C_T^2 / T^2$$

Reitebuch, O., 1999: SODAR-Signalverarbeitung von Einzelpulsen zur Bestimmung hochaufgelöster Windprofile. Schriftenreihe des Fraunhofer-Instituts für Atmosphärische Umweltforschung, Shaker Verlag GmbH Aachen, Bd. 62, 178 S.

Tatarskii, V.I., 1971: The effect of the turbulent atmosphere on wave propagation. Kefer Press, Jerusalem, 472 S.

SODAR sample plot (daytime convective BL)

acoustic backscatter intensity

sigma w

40 – 300 m

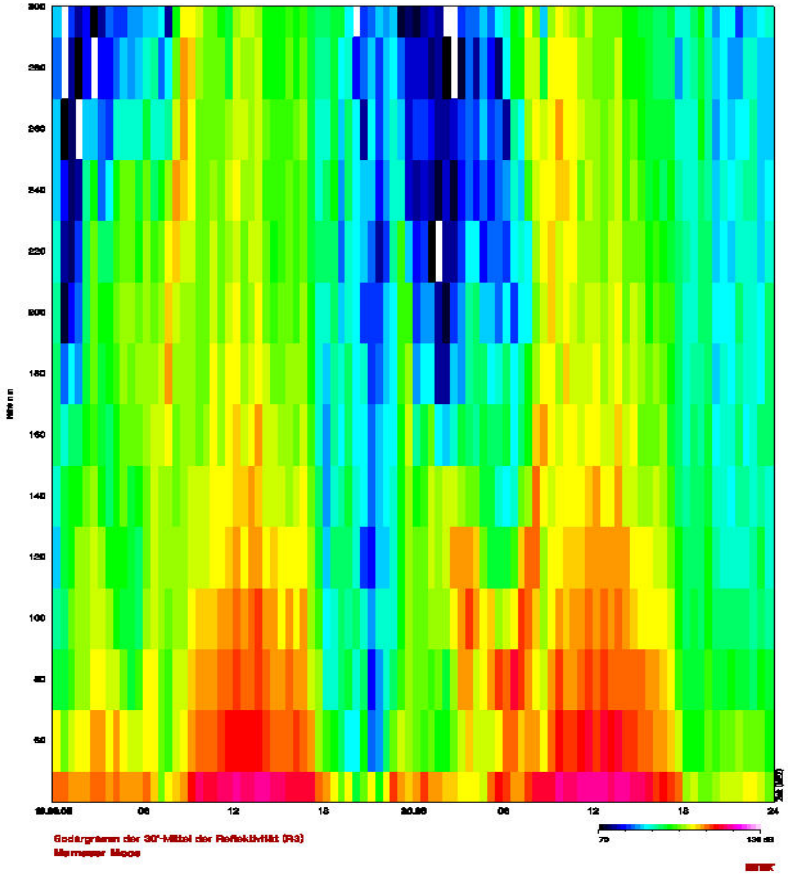

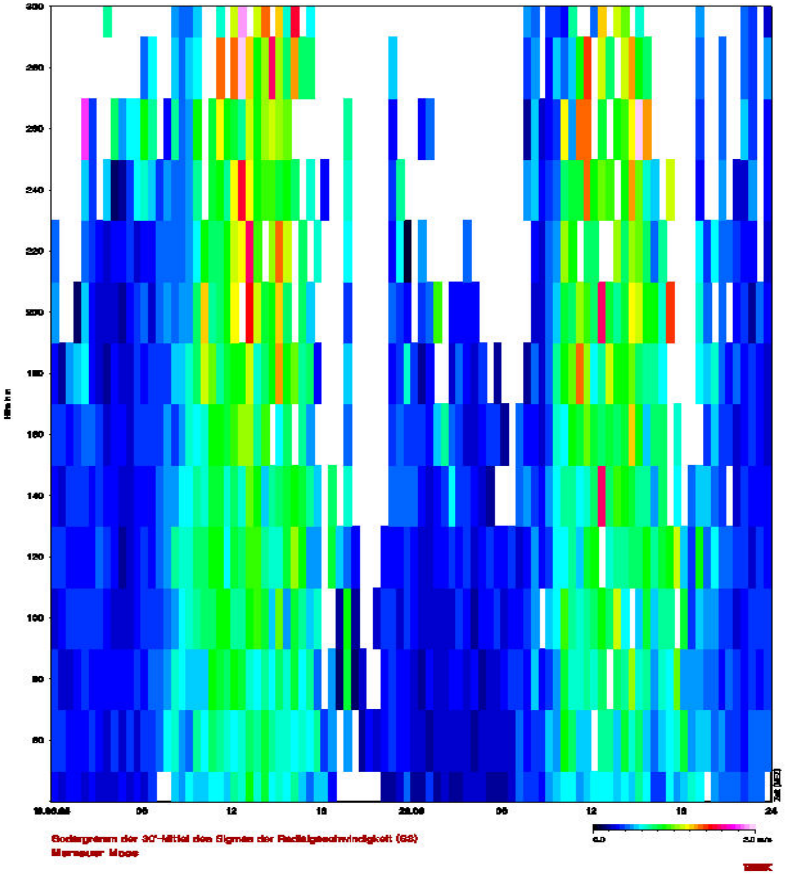

2 days, midnight to midnight

SODAR sample plot (lifted inversion)

acoustic backscatter intensity

sigma w

40 – 400 m

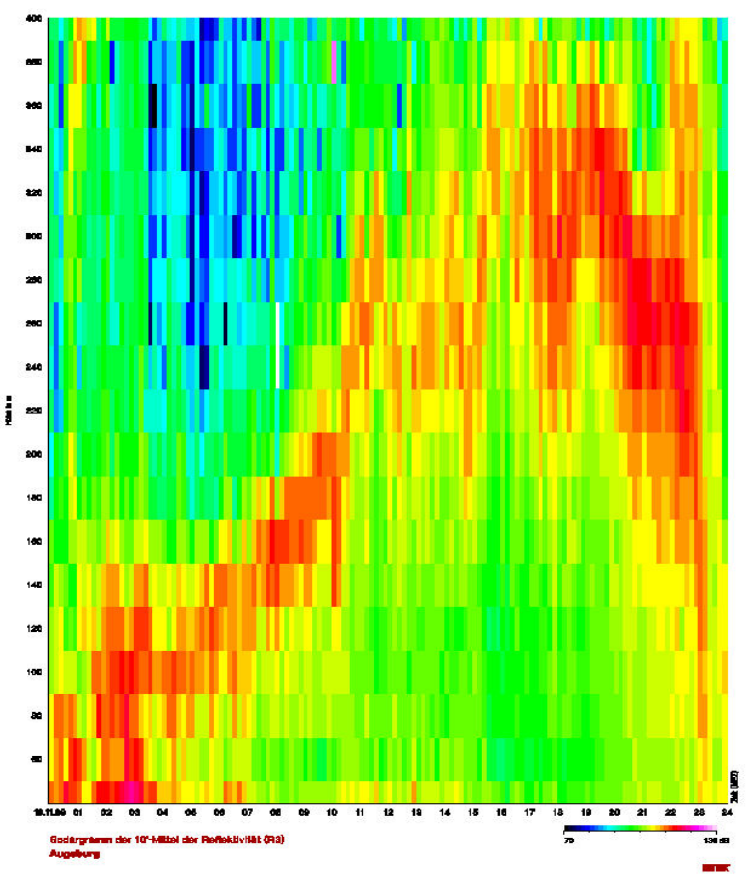

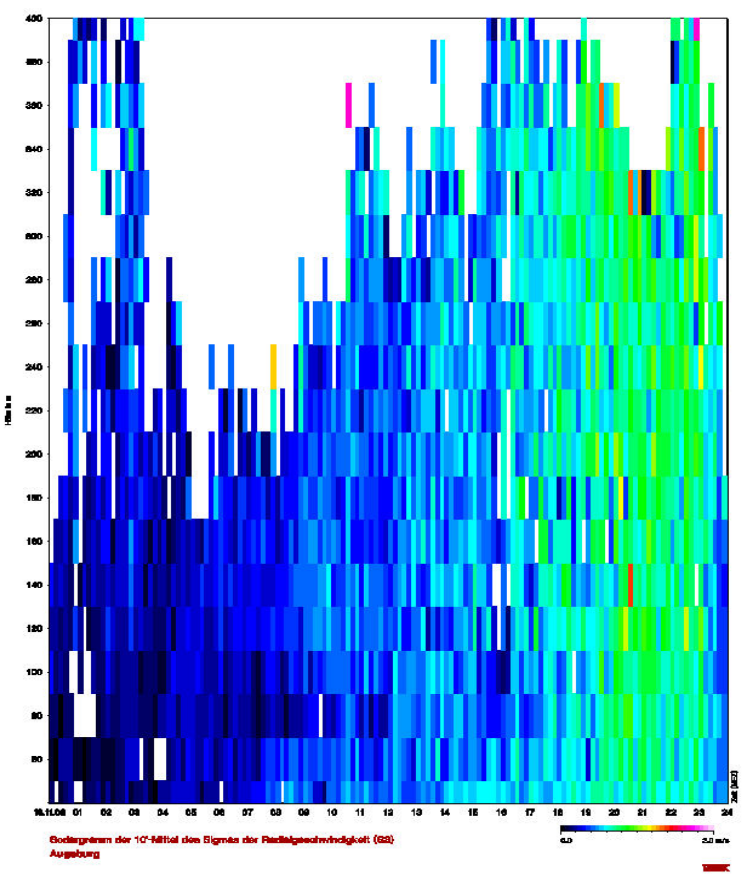

1 day, midnight to midnight

Algorithms to detect MLH from SODAR data

criterion 1:
upper edge of high turbulence

criterion 2:
surface and lifted inversions

MLH = Min (C1, C2)

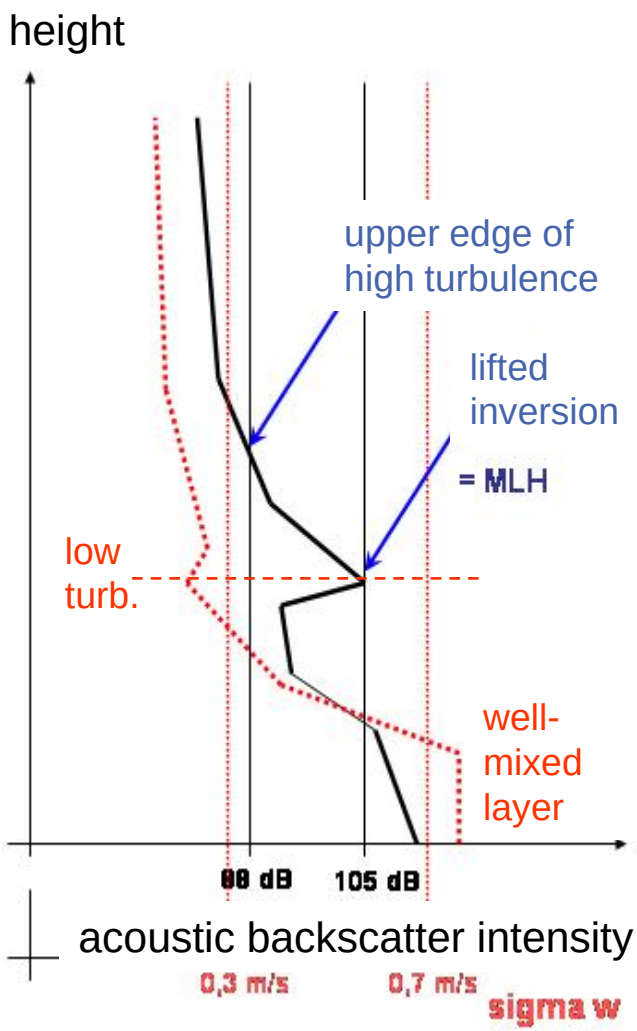

example 1: daytime

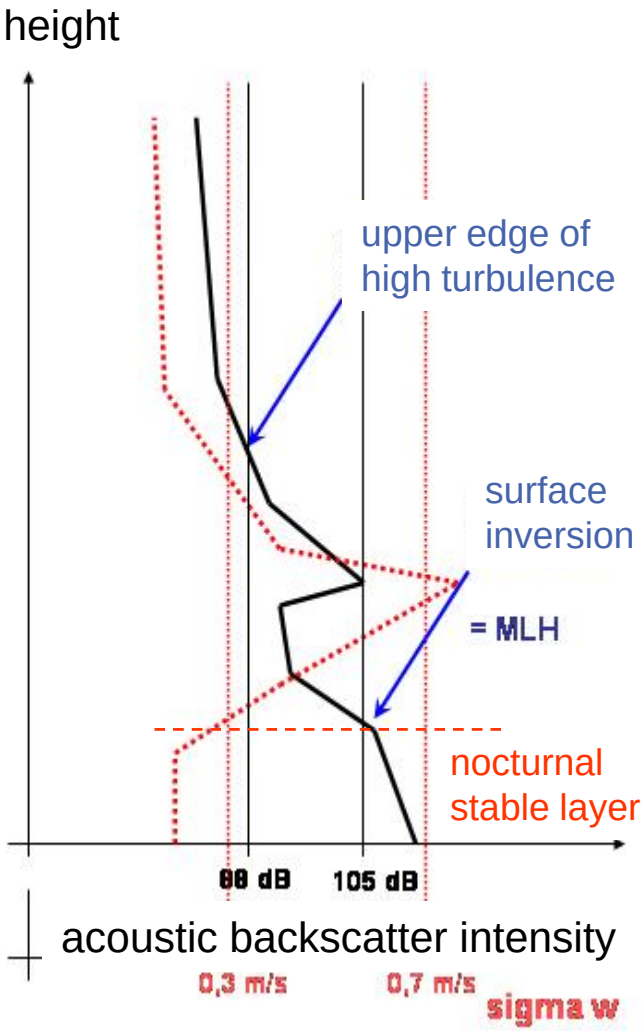

example 2: night-time

Ceilometer

algorithms for the determination of mixing-layer height

stefan.emeis@kit.edu Institute for Meteorology and Climate Research – Atmospheric Environmental Research

Ceilometer/LIDAR measuring principle

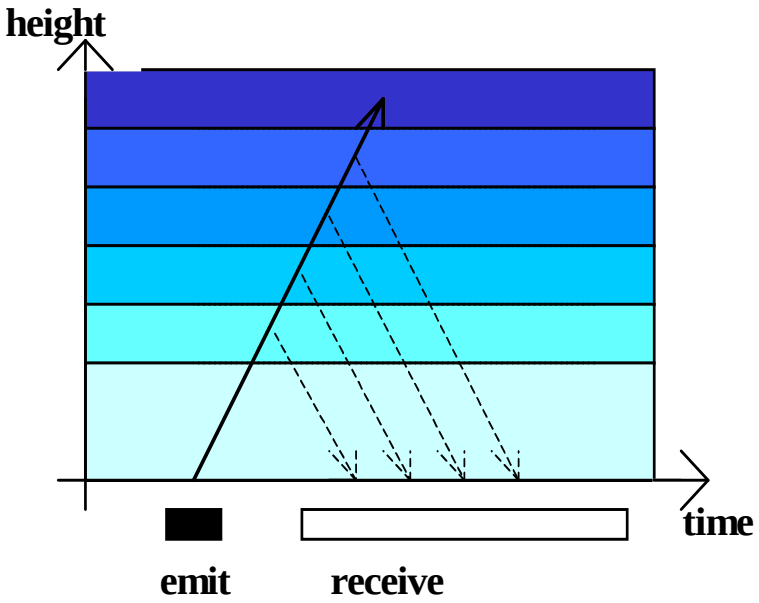

detection:

travel time of signal = height
backscatter intensity = particle size and number distribution
Doppler-shift = cannot be analyzed from ceilometer data
(available only from a Wind-LIDAR: velocity component in line of sight)

The LIDAR equation:

$$P_R(\lambda,r) = r^{-2}\,(c\tau A\varepsilon/2)\,P_0\,[\beta_m(\lambda,r) + \beta_p(\lambda,r)]\,e^{-2\sigma r} + P_{bg}$$

- r distance between the LIDAR and the backscattering object,
- c speed of light,
- τ pulse duration,
- A antenna area,
- ε correction term for the detector efficiency and losses due to the lenses,
- P_0 emitted energy,
- β_m backscatter coefficient for molecules
- β_p backscatter coefficient for particles,
- σ absorption of light in the atmosphere,
- P_{bg} background noise.

For a ceilometer β_m is negligible and only β_p is important

ceilometer sample plot (daytime convective BL)

optical backscatter intensity

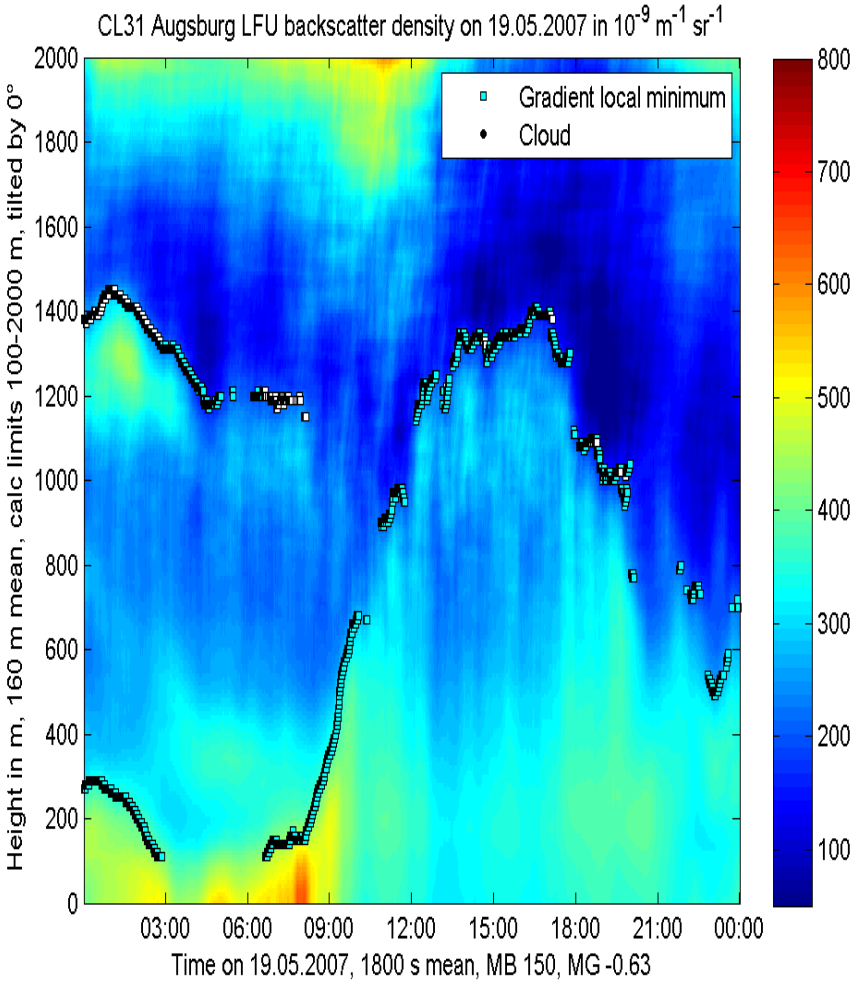

negative vertical gradient of optical backscatter intensity

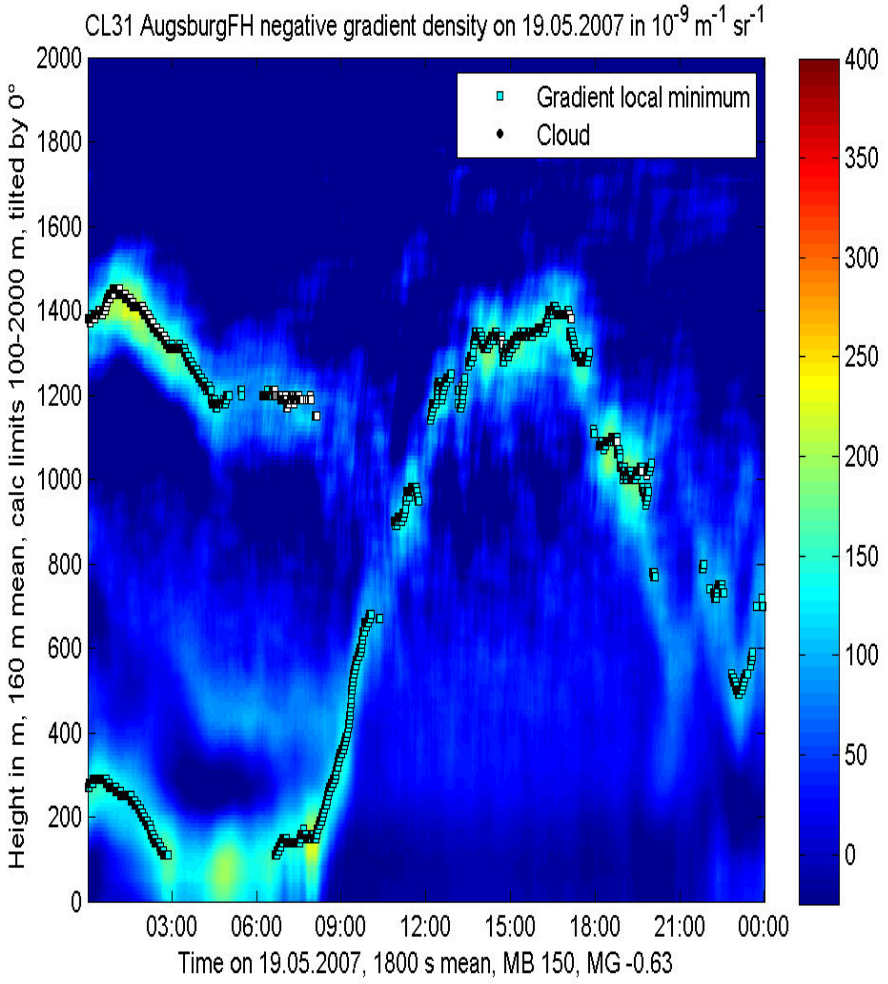

Algorithm to detect MLH from Ceilometer-Daten

criterion

minimal vertical gradient of backscatter intensity (the most negative gradient)

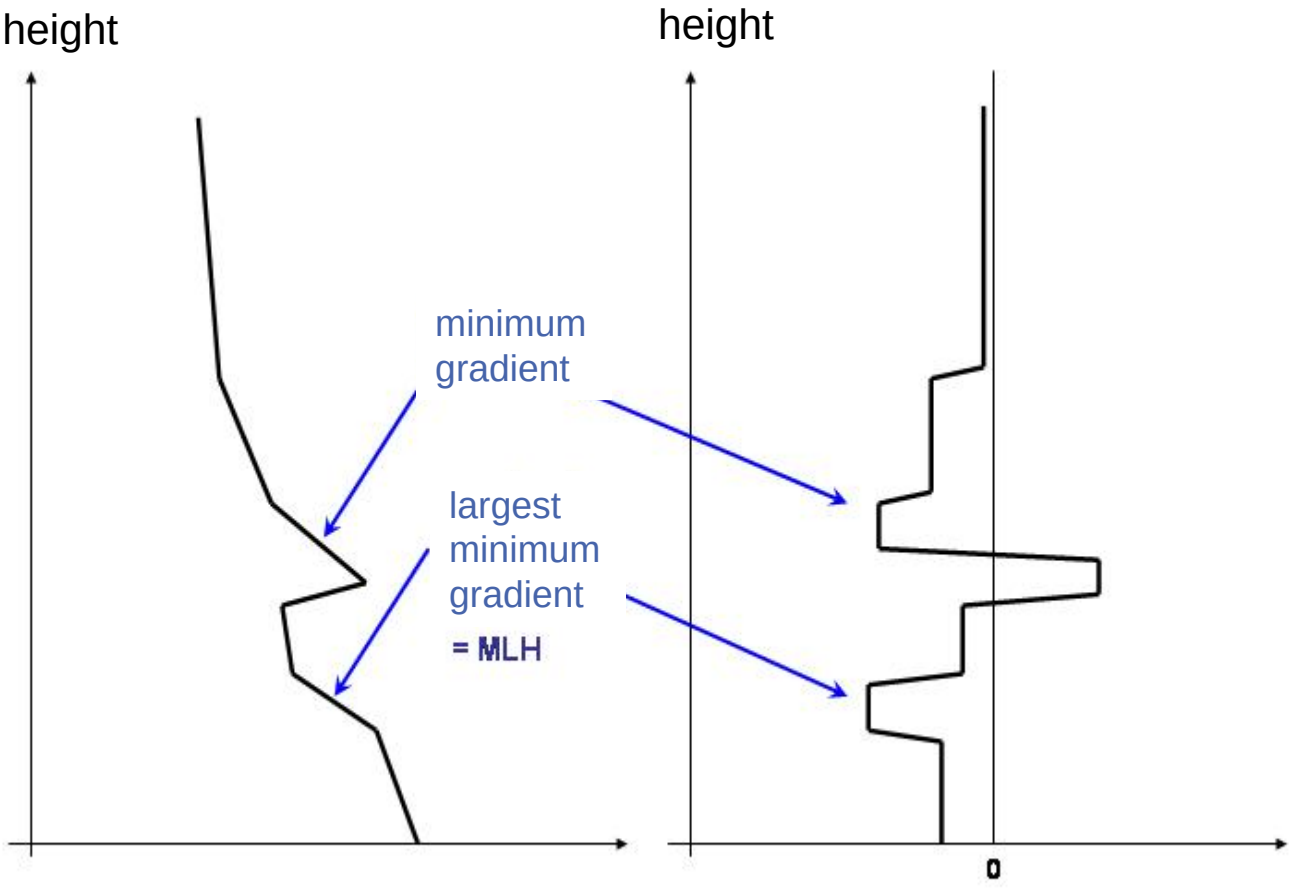

Different gradient methods (see Sicard et al. 2006, BLM 119, 135-157)

logarithmic gradient minimum

gradient minimum

inflection point method
(minimum of 2nd derivative)

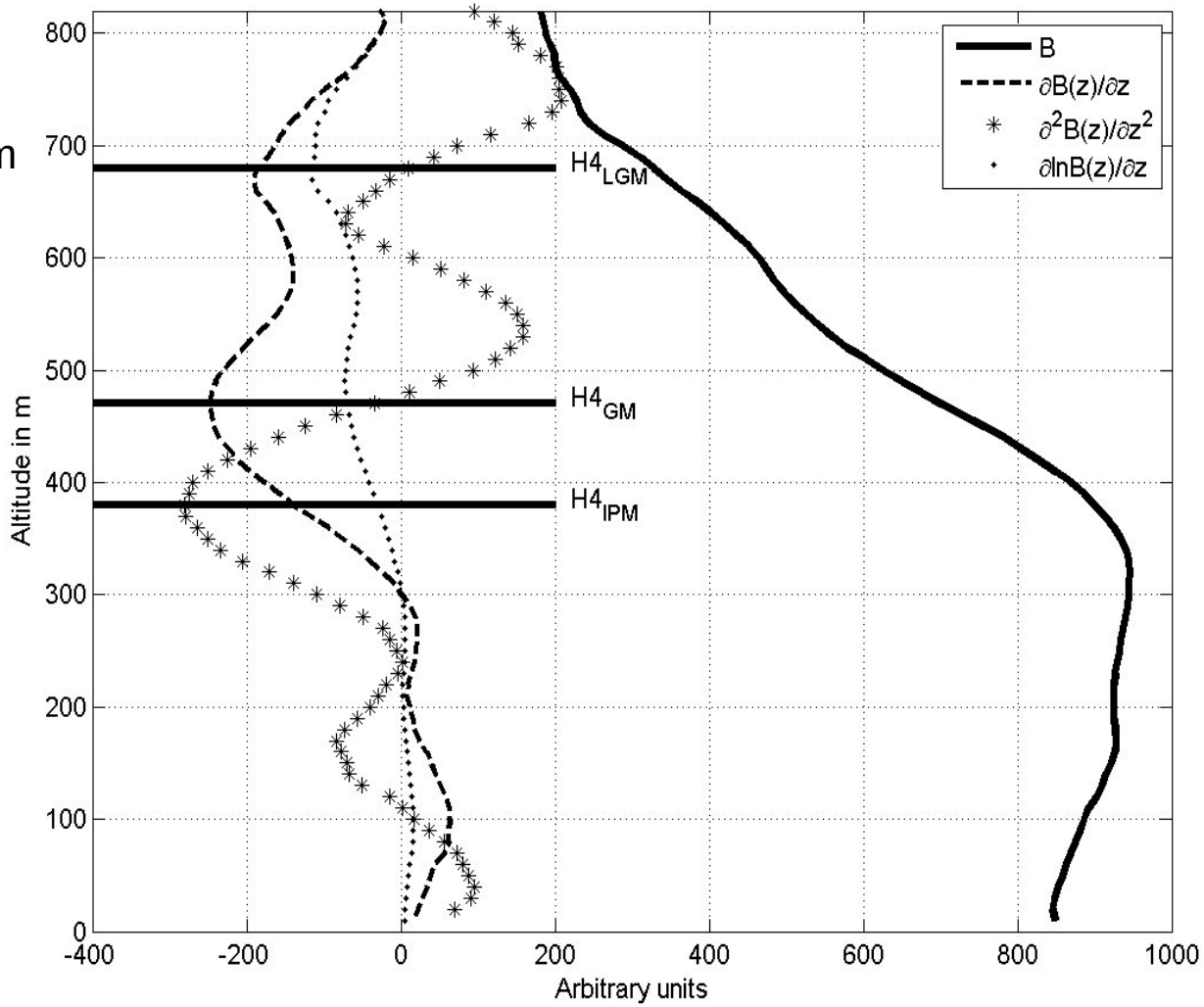

comparison of two different ceilometers

LD40

two optical axes
- wave length: 855 nm
- height resolution: 7.5 m
- max. range: 13000 m

CL31

one optical axis
- wave length: 905 nm
- height resolution: 5 m
- max. range: 7500 m

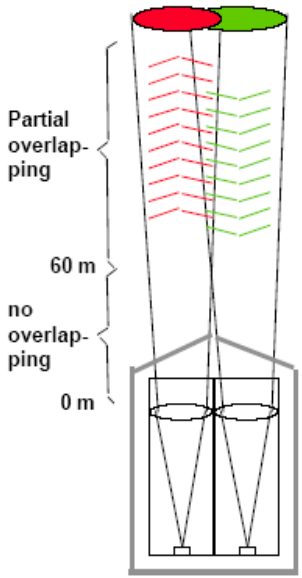

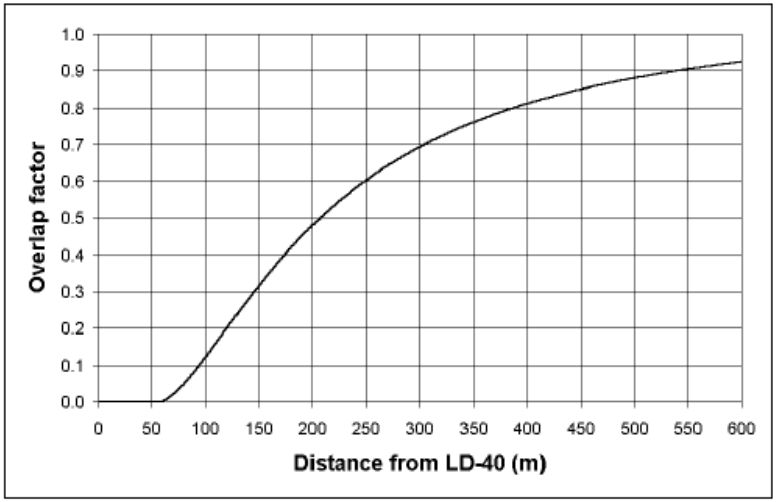

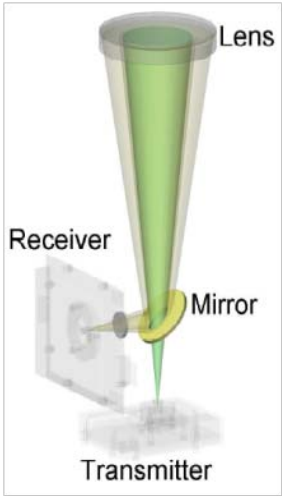

comparison of LD40 and CL31

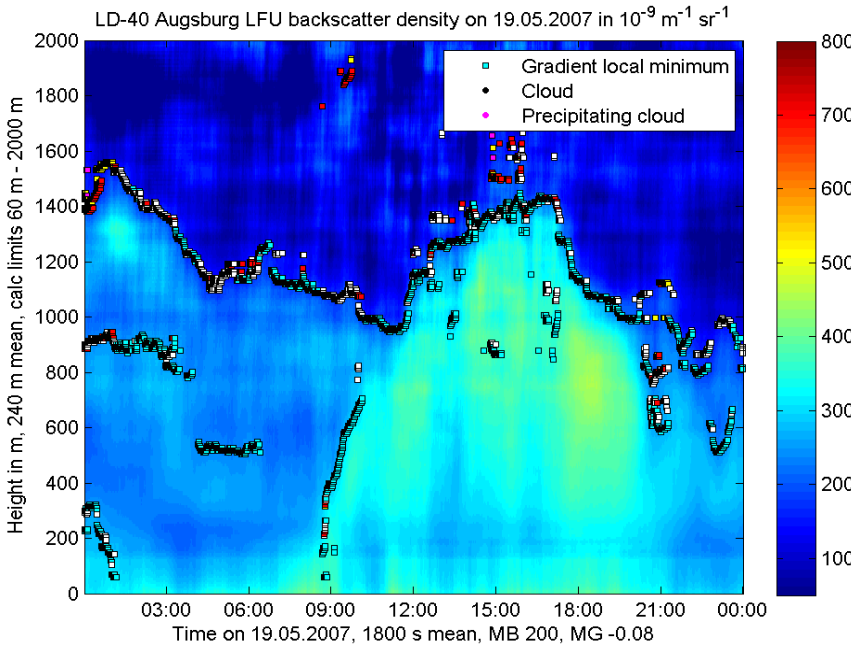

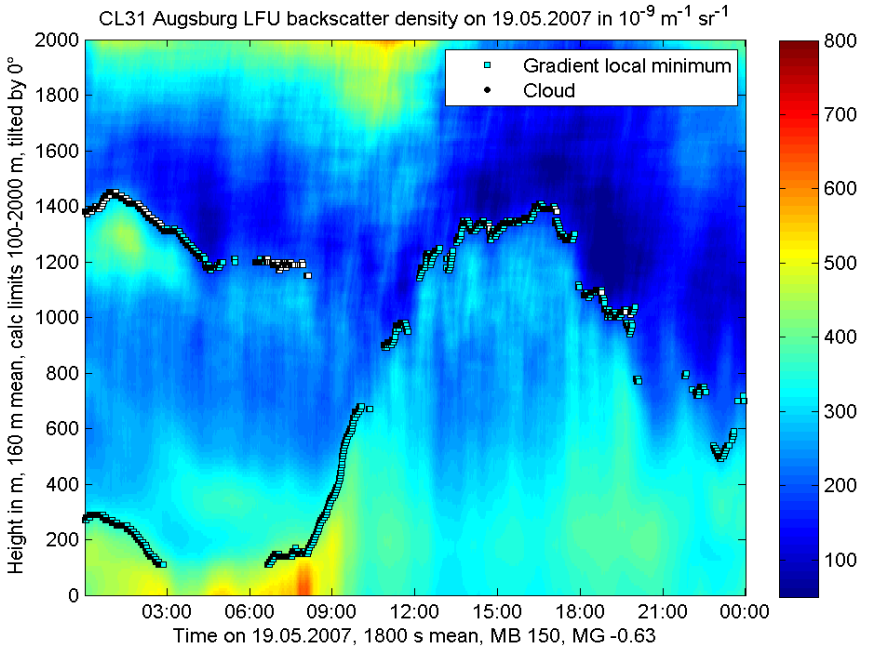

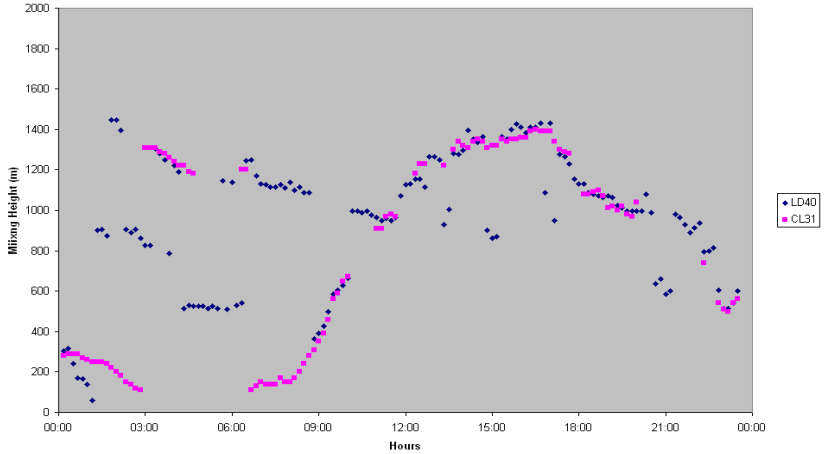

Eyjafjallajökull ash cloud over Southern Germany

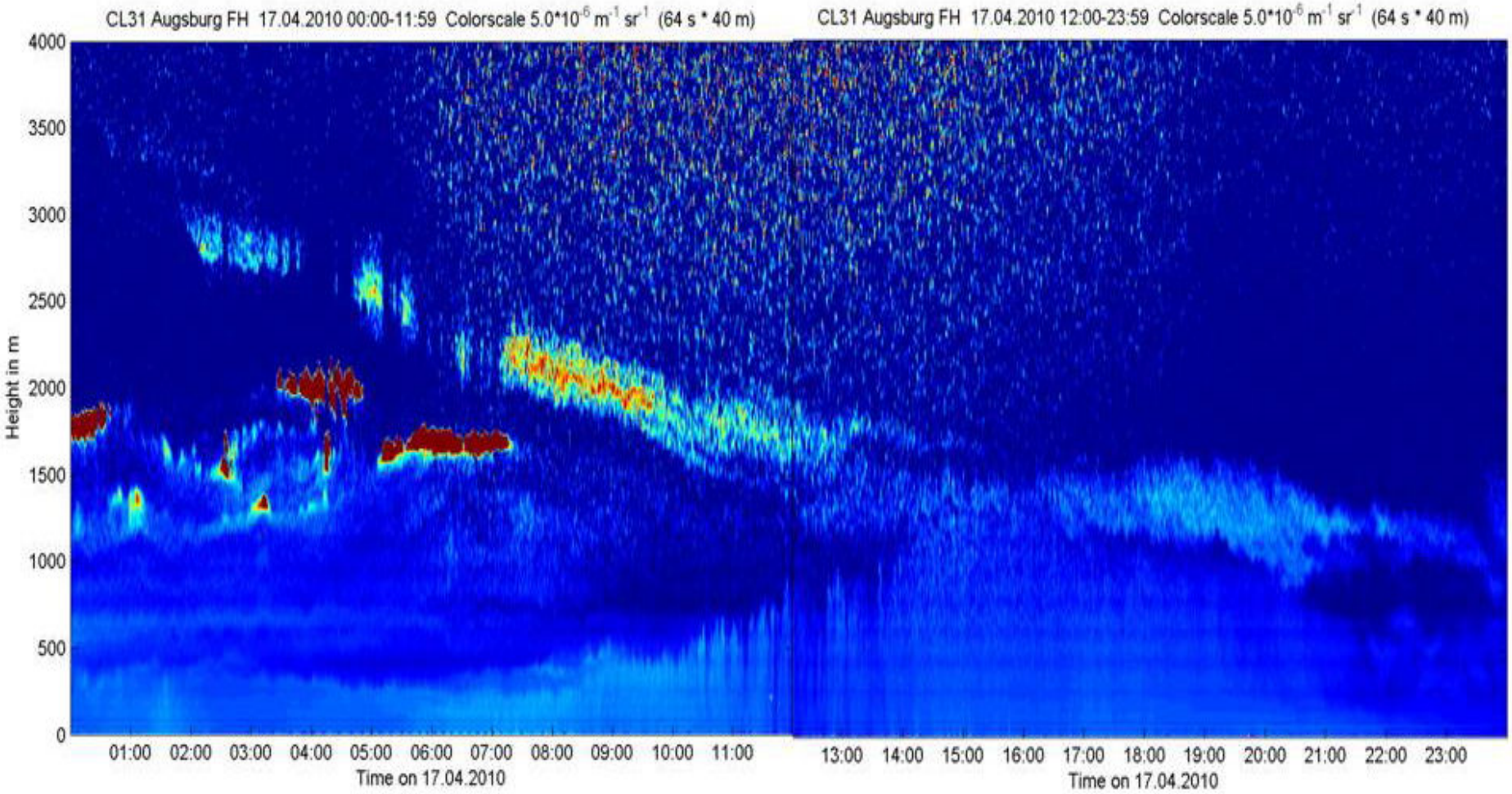

Application examples for SODAR and Ceilometer

stefan.emeis@kit.edu Institute for Meteorology and Climate Research – Atmospheric Environmental Research

Detection of multiple layering
Ceilometer and SODAR observations from an Alpine valley

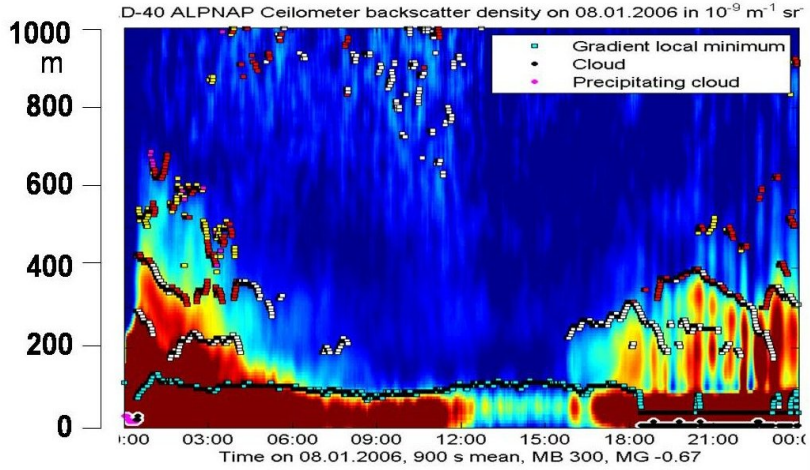

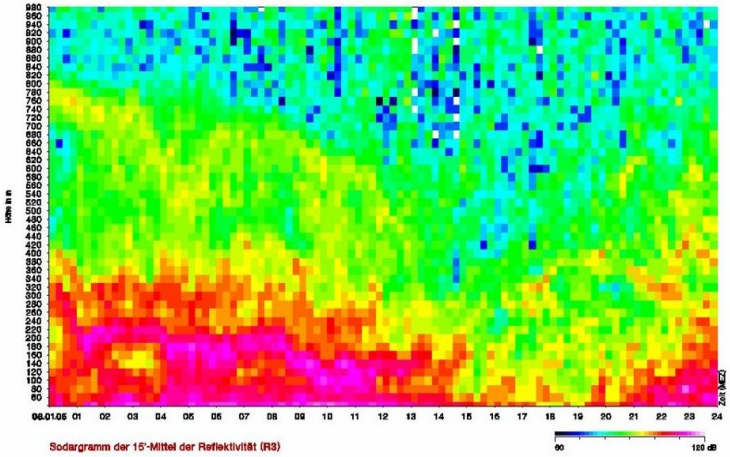

optical backscatter intensity

acoustic backscatter intensity

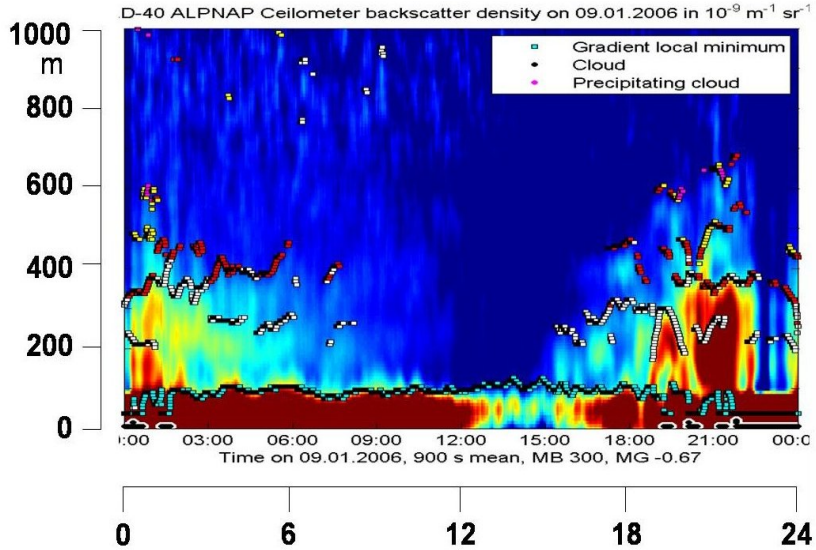

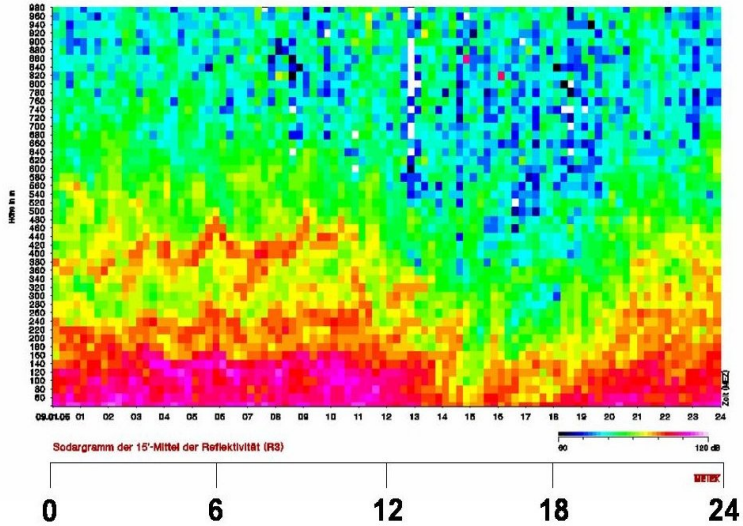

Detection of the diurnal variation of PBL structure from SODAR and Ceilometer data taken in Budapest

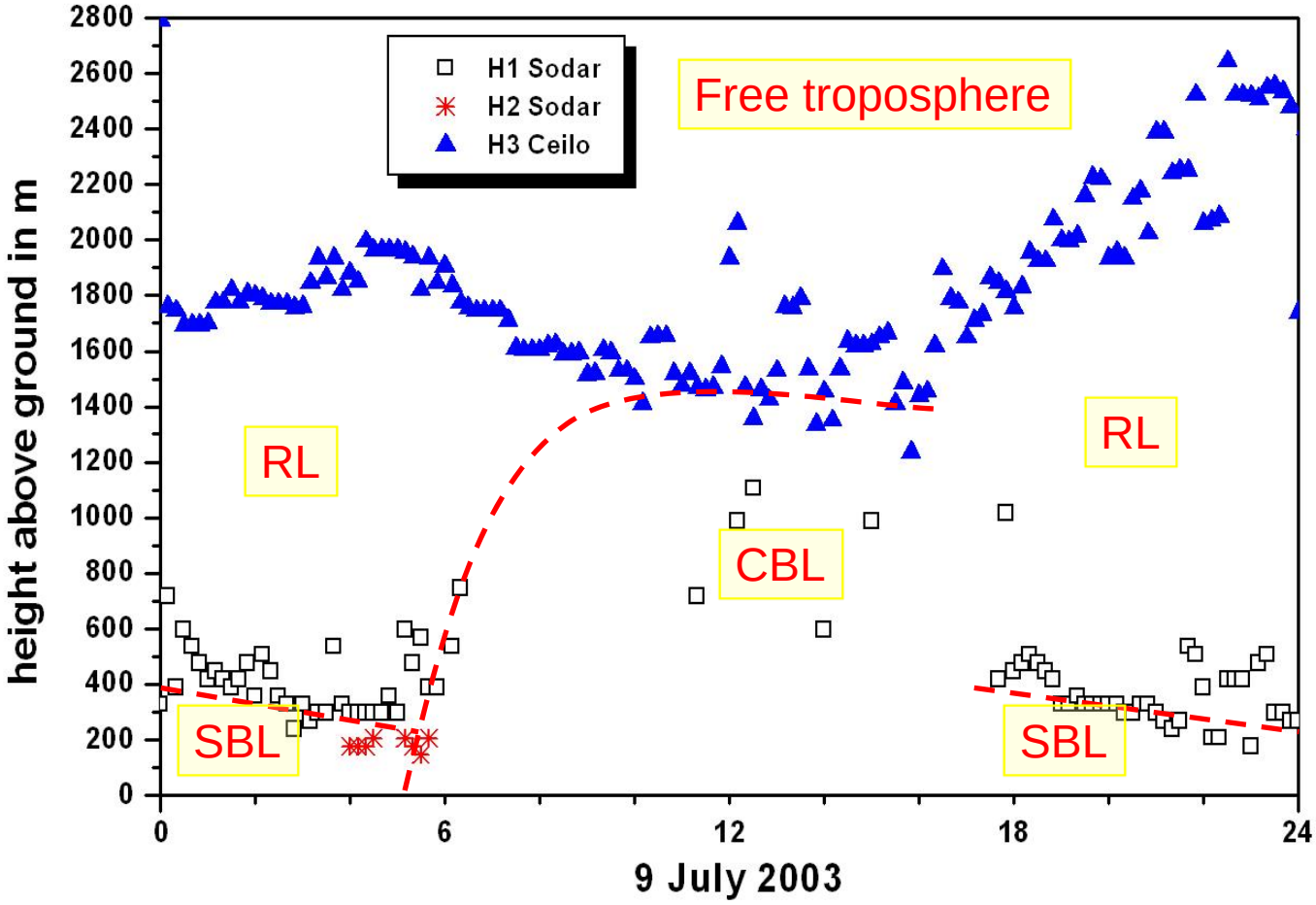

SBL:

stable boundary layer (usually at night and in winter)

CBL:

convective boundary layer (usually at daytime due to strong insolation)

RL:

residual layer (usually at nighttime)

Emeis, S., K. Schäfer, 2006: Remote sensing methods to investigate boundary-layer structures relevant to air pollution in cities. Bound.-Lay Meteorol., 121, 377-385,

Differences in MLH detection from SODAR and Ceilometer data taken in Budapest

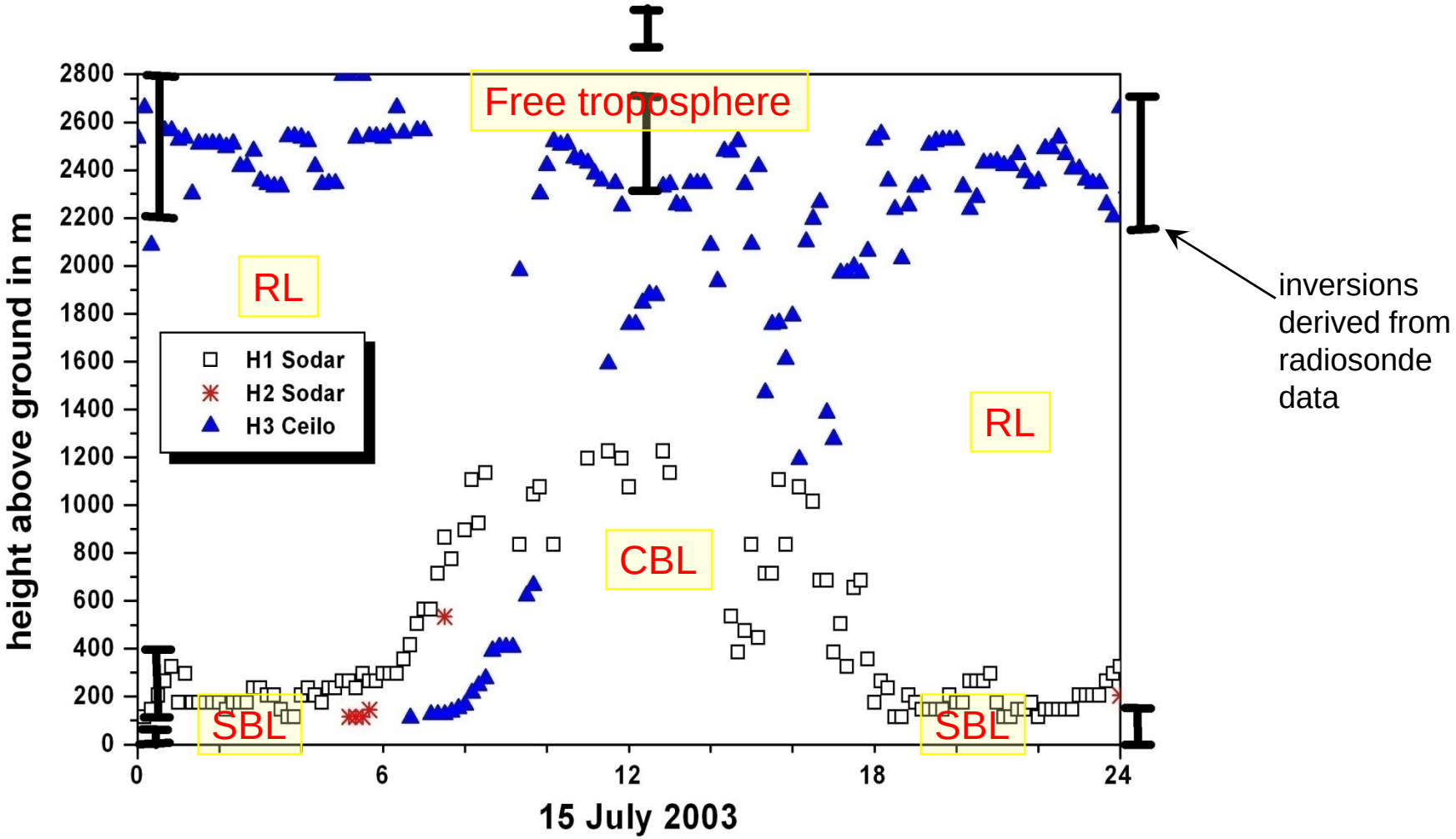

Emeis, S., K. Schäfer, 2006: Remote sensing methods to investigate boundary-layer structures relevant to air pollution in cities. Bound.-Lay Meteorol., 121, 377-385,

RASS

principles of operation

examples

stefan.emeis@kit.edu Institute for Meteorology and Climate Research – Atmospheric Environmental Research

RASS (radio-acoustic remote sensing)

measures vertical temperature profiles

Bragg-RASS: windprofiler plus acoustic component

Doppler-RASS: SODAR plus electro-magnetic component

UHF RASS (boundary layer)

VHF RASS (troposphere)

RASS: frequencies

Bragg condition:
acoustic wavelength = ½ electro-magnetic wavelength

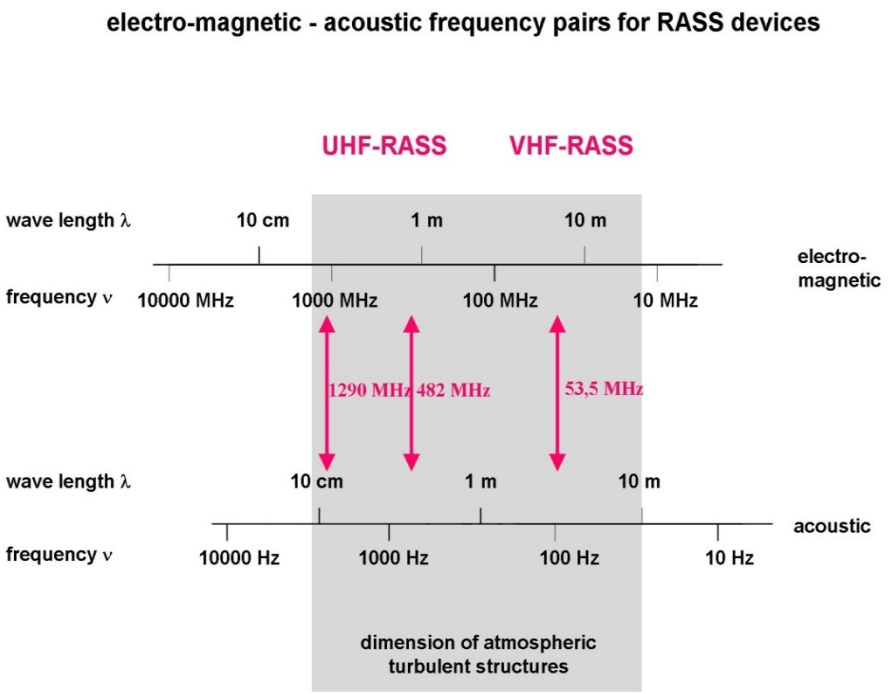

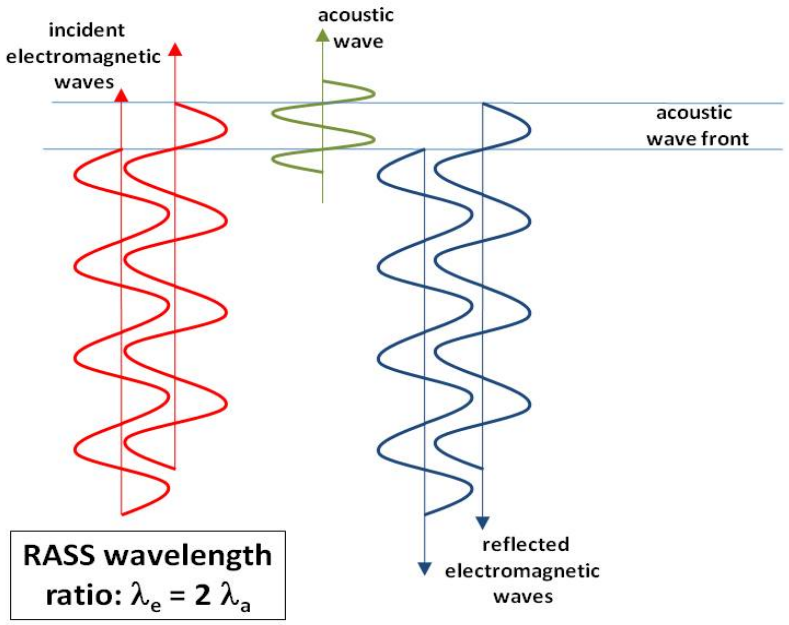

Emeis, S., 2010: Measurement Methods in Atmospheric Sciences - In situ and remote. Borntraeger, Stuttgart, 272 pp., 103 figs, 28 tables, ISBN 978-3-443-01066-9.

SODAR-RASS
(Doppler-RASS)

(METEK)

acoustic frequ.: 1500 – 2200 Hz
radio frequ.: 474 MHz
resolution: 20 m
lowest
range gate: ca. 40 m

vertical range: 540 m

Bragg-RASS

acoustic frequ.: about 3000 Hz
radio frequ.: 1290 MHz
resolution: 50 m
lowest
range gate: ca. 200 m

vertical range: 1000 m

example RASS data: summer day
potential temperature (left), horizontal wind (right)

300 m

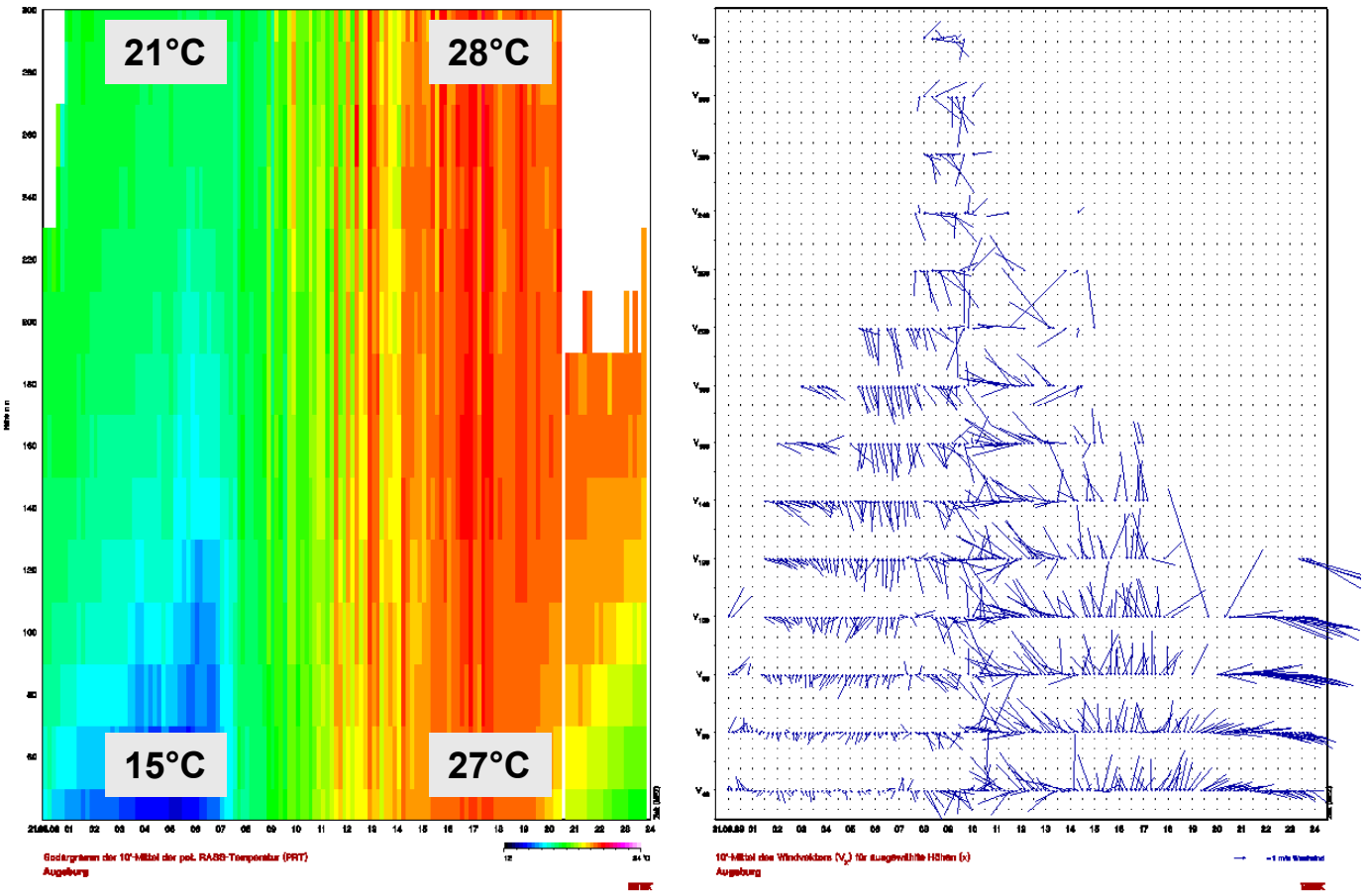

40 m

example RASS data: winter day
potential temperature (left), horizontal wind (right)

300 m

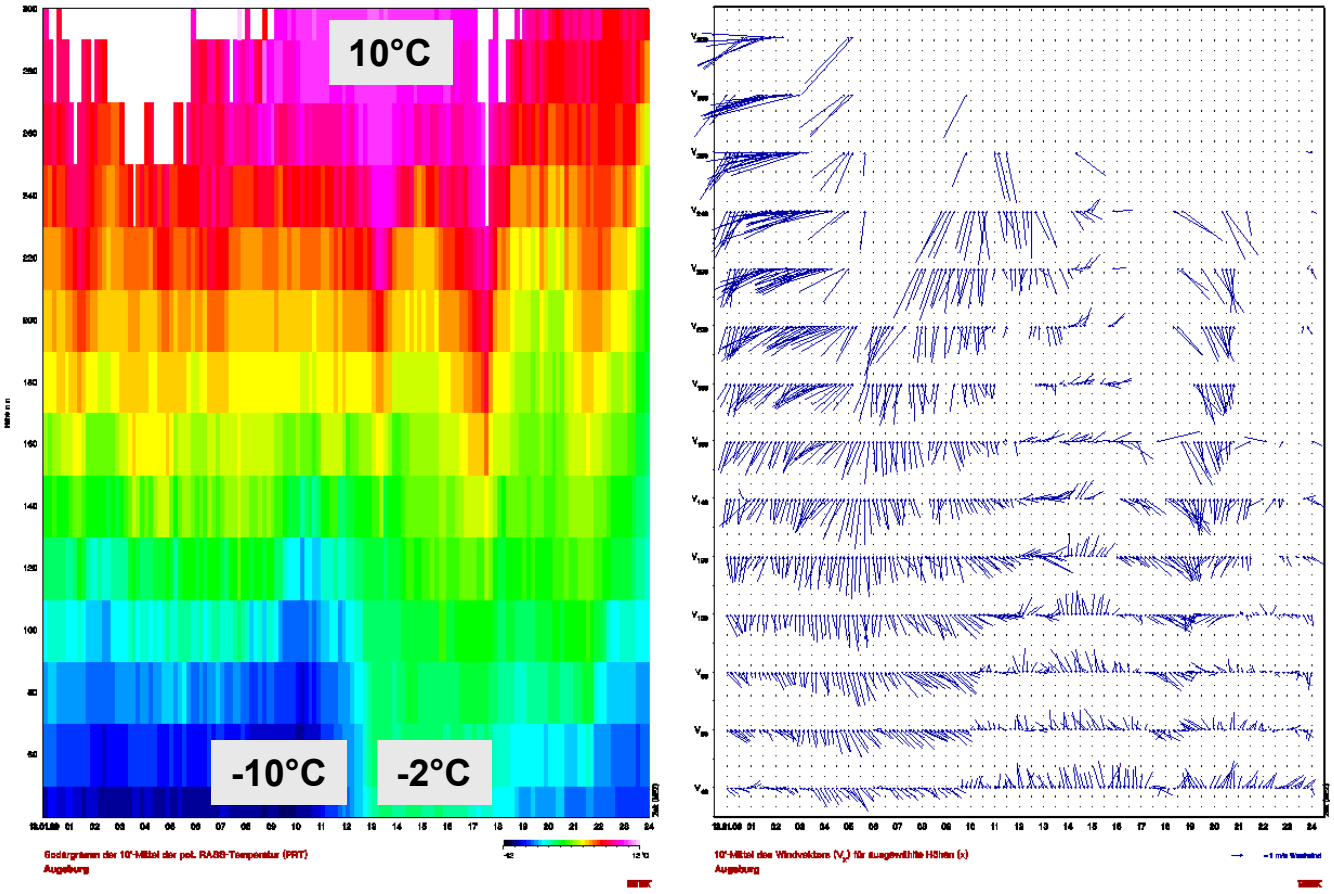

40 m

example RASS data: inversion
potential temperature (left), horizontal wind (right)

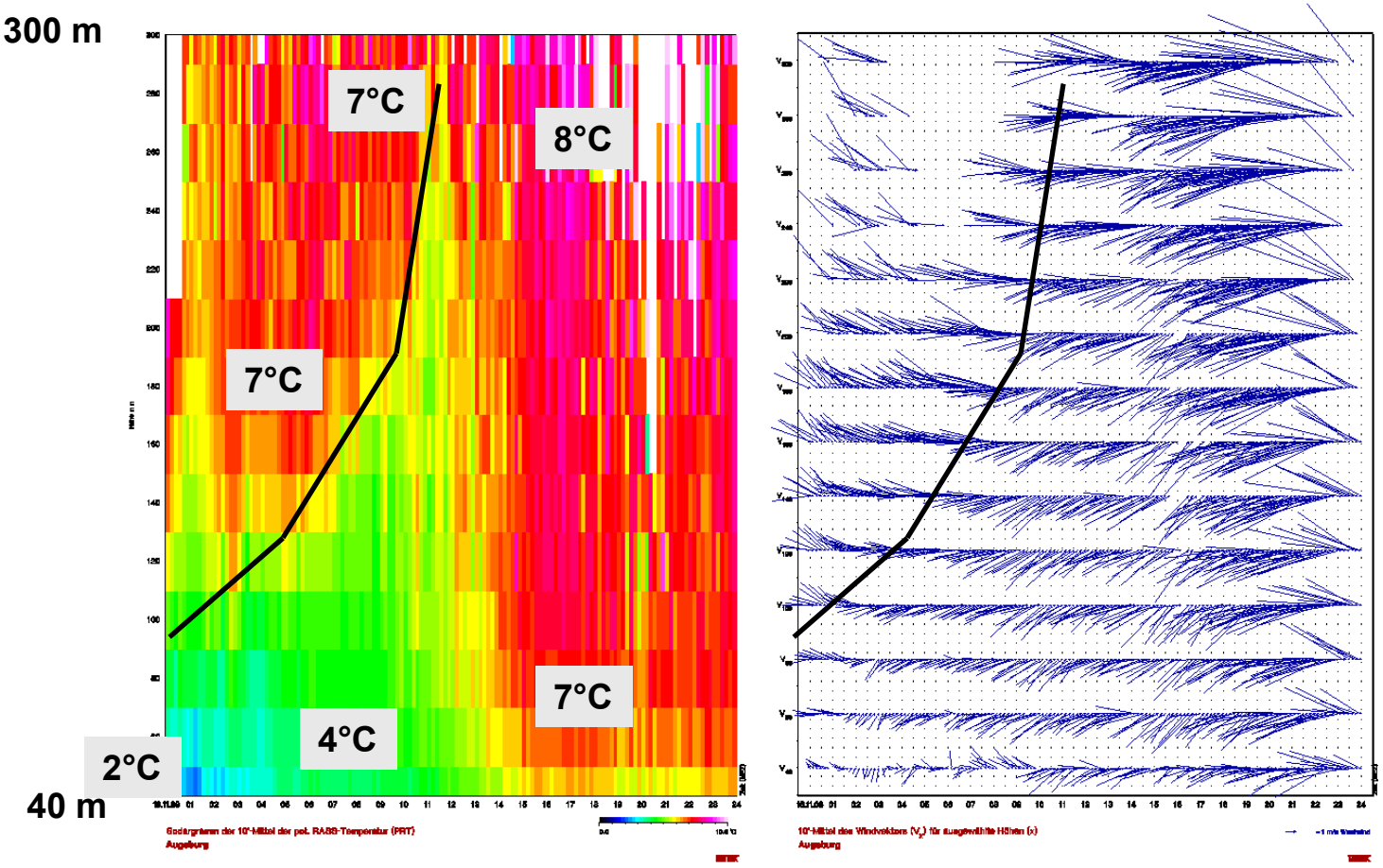

temperature profile and pollution

comparison of RASS data (potential temperature, right) with aerosol backscatter from a ceilometer (left)

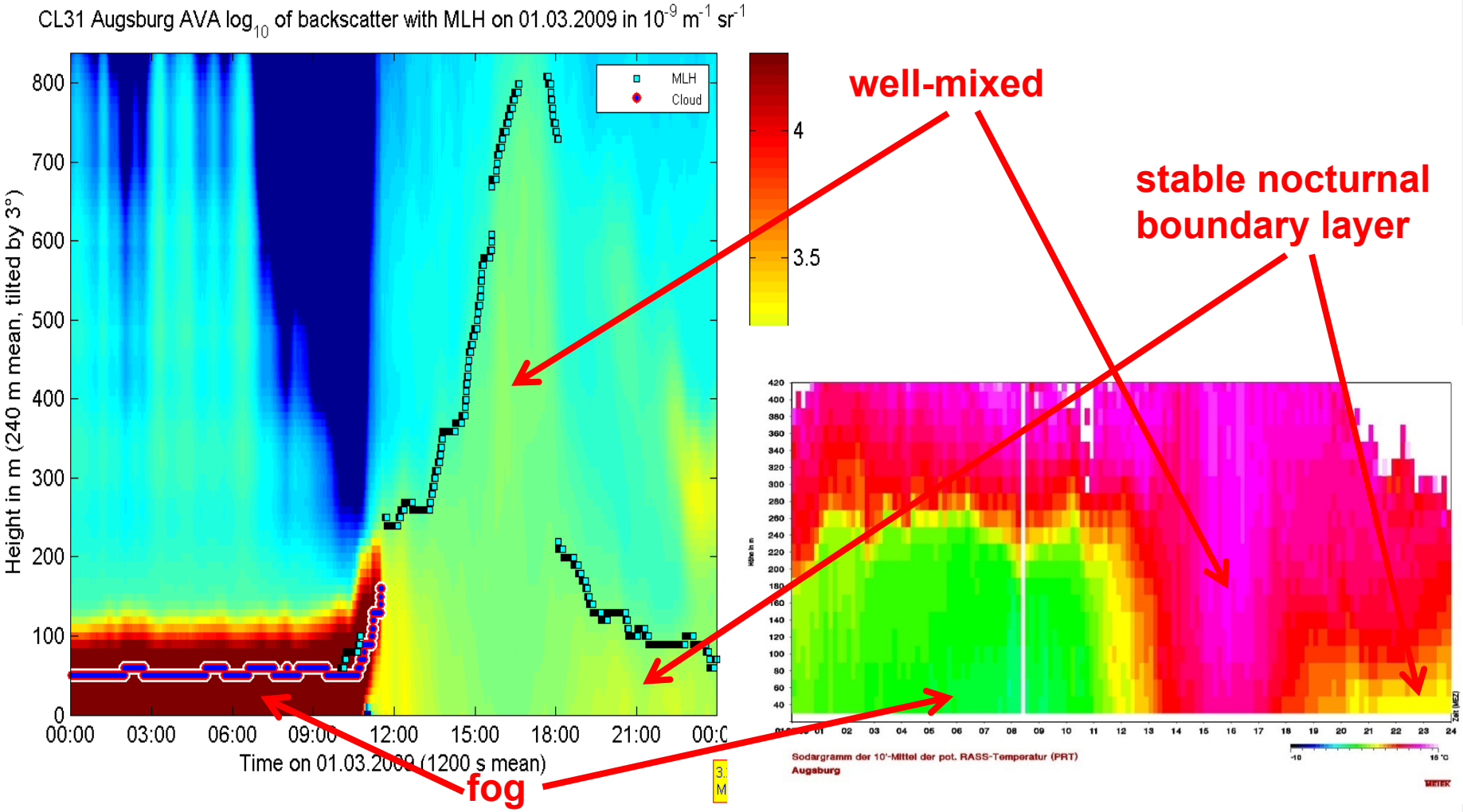

RASS data Augsburg February 2009

potential temperature (top), backscatter SODAR (middle), Ceilometer (bottom)

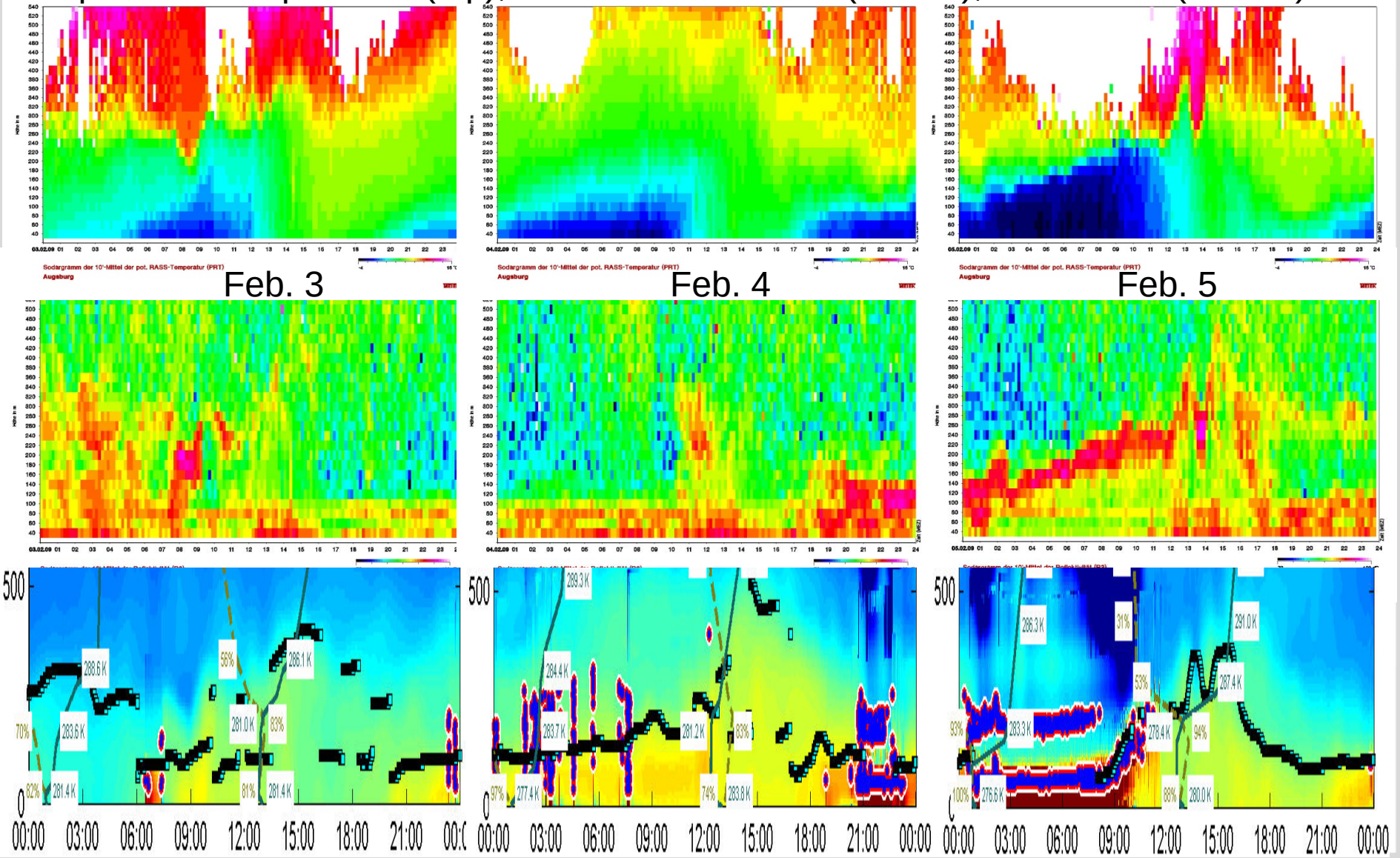

RASS data Augsburg February 2009

potential temperature (top), MLH RASS (middle), MHL SODAR/Ceilo (bottom)

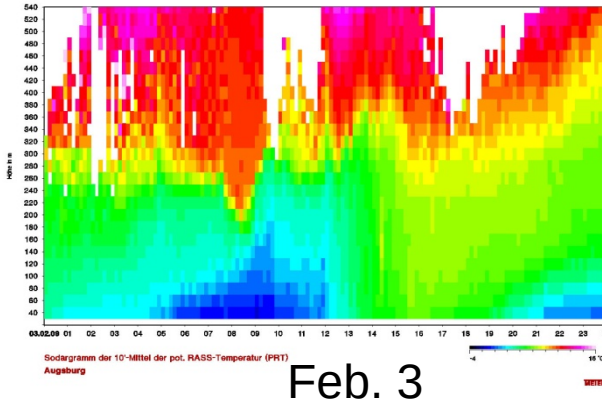

Feb. 3

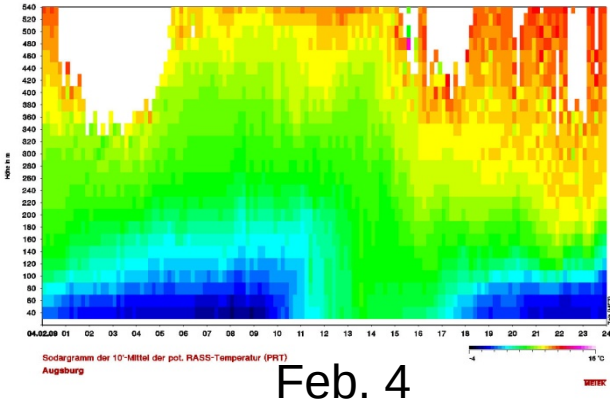

Feb. 4

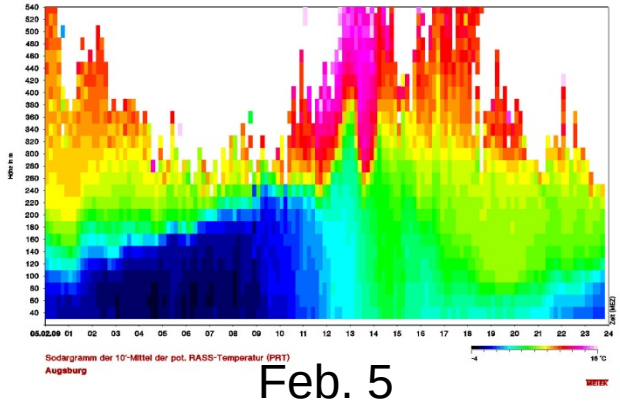

Feb. 5

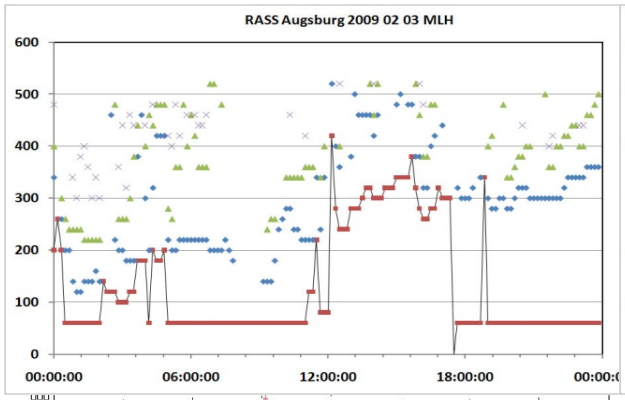

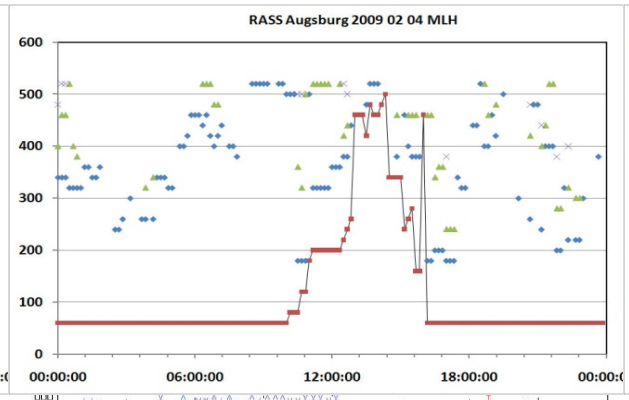

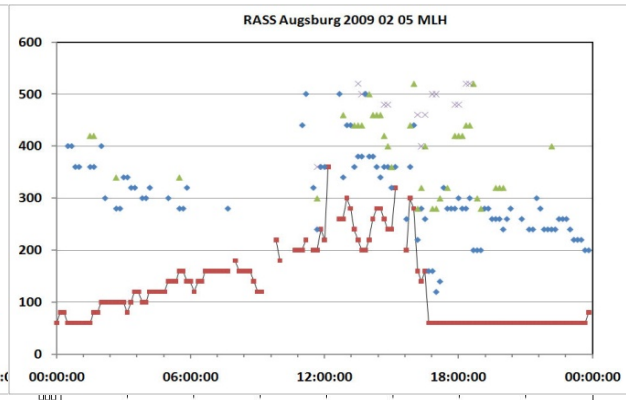

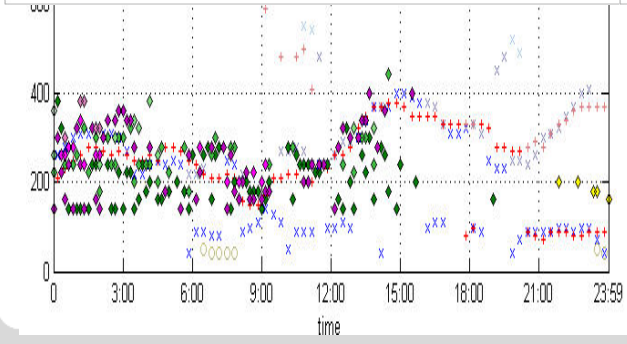

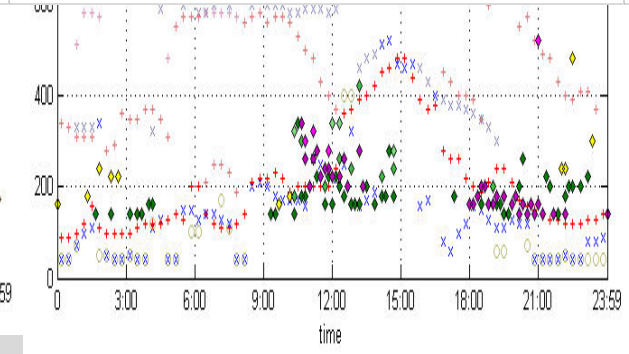

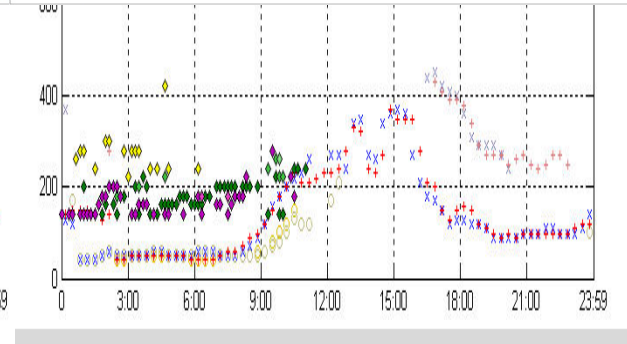

Summary

Overview on methods using ground-based remote sensing for the derivation of the mixing-layer height

method		short description
acoustic	ARE method	analysis of **a**coustic **r**eceived **e**cho intensity profiles
"	HWS method	analysis of **h**orizontal **w**ind **s**peed profiles
"	VWV method	analysis of **v**ertical **w**ind **v**ariance profiles
"	EARE method	analysis of acoustic backscatter intensity and vertical wind variance profiles (**e**nhanced **a**coustic **r**eceived **e**cho method)
optical	threshold method	detection of a given backscatter intensity threshold
"	gradient method	analysis of optical backscatter intensity profiles
"	idealised backscatter method	analysis of optical backscatter intensity profiles
"	wavelet method	analysis of optical backscatter intensity profiles
"	variance method	analysis of optical backscatter intensity profiles
acoustic / electro-magnetic		ARE method applied to sodar and wind profiler data
acoustic / optical		EARE method plus gradient method
electro-magnetic / electro-magnetic		combination of a sodar-RASS and a wind profiler RASS: analysis of the vertical temperature profile plus analysis of the electro-magnetic backscatter intensity profile
acoustic / in situ		ARE method plus in-situ surface flux measurement

RASS	analysis of the temperature profile from the measured speed of sound

Conclusions:

☺ ☺ ☺ 💣 **RASS directly delivers temperature profiles, MLH, inversions, and stable layers can easily be detected, wind profiles are additionally available.**
Does not work properly under high wind speeds. Restricted range.

☺ ☺ 💣 💣 **Ceilometer detects aerosol distribution and water droplets. It has to be assumed that the aerosol follows the thermal structure of the atmosphere. Inversions and MLH can indirectly be inferred with a MLH algorithm.**
Does not work properly in extreme clear (aerosol-free) air and during precipitation events and fog.

☺ 💣 💣 💣 **SODAR detects temperature fluctuations and gradients, but no absolute temperature. Inversions and stable layers can indirectly be inferred with a MLH algorithm.**
Does not work properly under perfectly neutral stratification, with very high wind speeds, and during stronger precipitation events. Restricted range.

Literature

SODAR:

Asimakopoulos, D.N., C.G. Helmis, J. Michopoulos, 2004: Evaluation of SODAR methods for the determination of the atmospheric boundary layer mixing height. - Meteor. Atmos. Phys. 85, 85–92.

Beyrich, F., 1997: Mixing height estimation from sodar data – a critical discussion. - Atmos. Environ. 31, 3941–3953.

Ceilometer:

Schäfer, K., S.M. Emeis, A. Rauch, C. Münkel, S. Vogt, 2004: Determination of mixing-layer heights from ceilometer data. In: Remote Sensing of Clouds and the Atmosphere IX. Schäfer, K., A. Comeron, M. Carleer, R.H. Picard, N. Sifakis (Eds.), Proc. SPIE, Bellingham, WA, USA, Vol. 5571, 248–259.

Sicard, M., C. Pérez, F. Rocadenbosch, J.M. Baldasano, D. García-Vizcaino, 2006: Mixed-Layer Depth Determination in the Barcelona Coastal Area From Regular Lidar Measurements: Methods, Results and Limitations. - Bound.-Lay. Meteor. 119, 135–157.

RASS:

Engelbart, D.A.M., J. Bange, 2002: Determination of boundary-layer parameters using wind profiler/RASS and sodar/RASS in the frame of the LITFASS project. Theor. Appl. Climatol. 73, 53–65.

Emeis, S., K. Schäfer, C. Münkel, 2009: Observation of the structure of the urban boundary layer with different ceilometers and validation by RASS data. Meteorol. Z., 18, 149-154. (Open access, freely available from http://dx.doi.org/10.1127/0941-2948/2009/0365)

Reviews:

Emeis, S., K. Schäfer, C. Münkel, 2008: Surface-based remote sensing of the mixing-layer height – a review. - Meteorol. Z., 17, 621-630. (Open access, freely available from http://dx.doi.org/10.1127/0941-2948/2008/0312)

Emeis, S., M. Harris, R.M. Banta, 2007: Boundary-layer anemometry by optical remote sensing for wind energy applications. - Meteorol. Z., 16, 337-347.

Thank you very much for your attention